School on Gravitational Waves, neutrinos and multiwavelenght e.m. observations: the new frontier of Astronomy

Coalescing binaries in Numerical Relativity 1 NS-NS

Toni Font (Universitat de València, Spain)

Outline

1. Introduction + motivation
2. Framework
3. Simulations
4. Summary

Suggested reading:

M. Alcubierre, "Introduction to 3+1 Numerical Relativity", Clarendon Press - Oxford (2007)

T.W. Baumgarte & S.L. Shapiro, "Numerical Relativity: Solving Einstein's equations on the computer", Cambridge University Press (2010)

J.A. Font, "Numerical hydrodynamics and magnetohydrodynamics in general relativity", Living Reviews in Relativity (2008) (www.livingreviews.org)

J.A. Faber & F.A. Rasio, "Binary neutron star mergers", Living Reviews in Relativity (2012) (www.livingreviews.org)

Why study binary neutron star mergers?

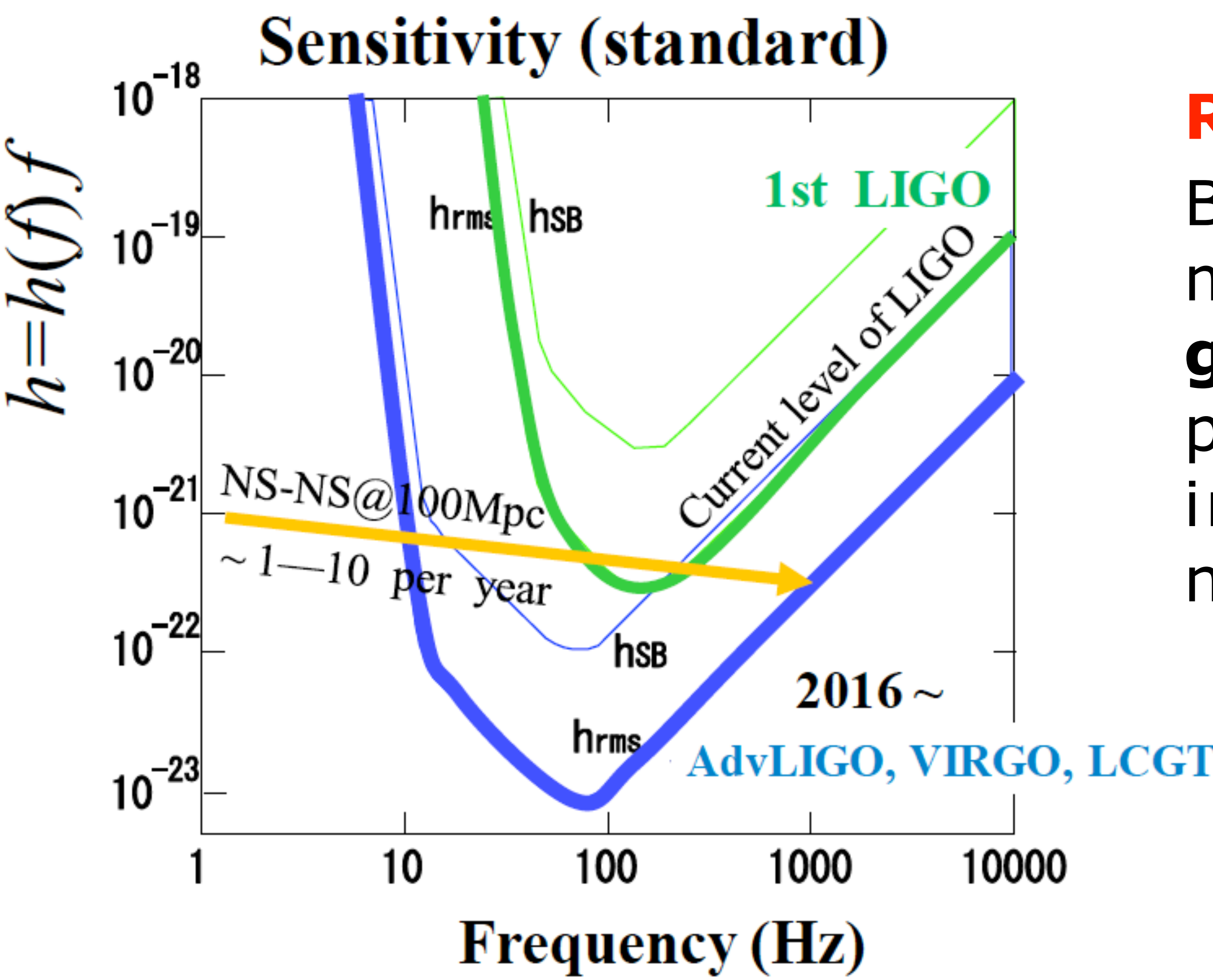

Reason #1:

Because they are among the most powerful sources of **gravitational waves.** Could provide key information to improve understanding of neutron star physics and EOS.

BNS & BH-NS mergers = GW source

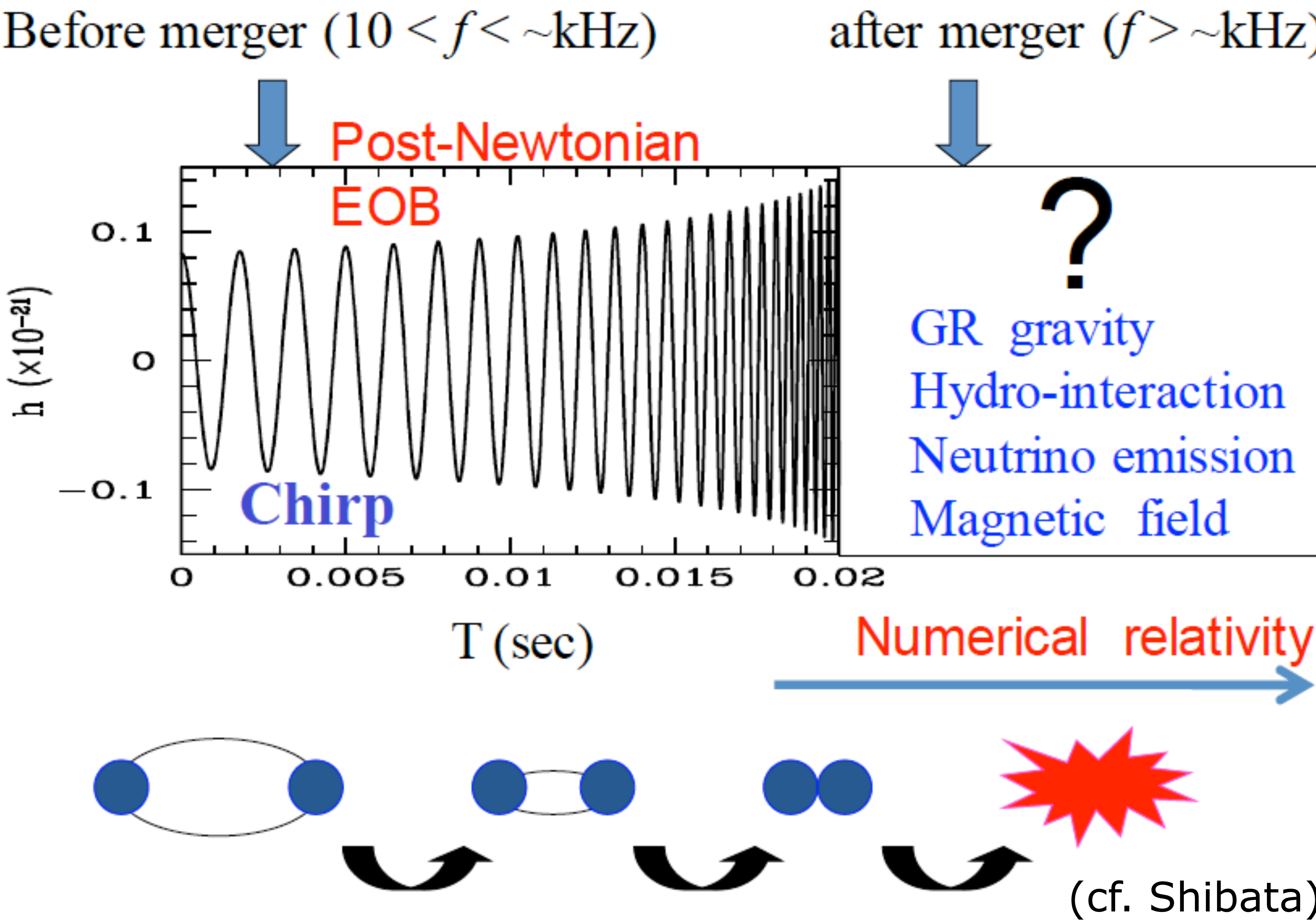

Why study binary neutron star mergers?

Reason #2: Excellent laboratory to study high-density nuclear physics (key to decipher the NS physics)

Neutron star composition still unknown

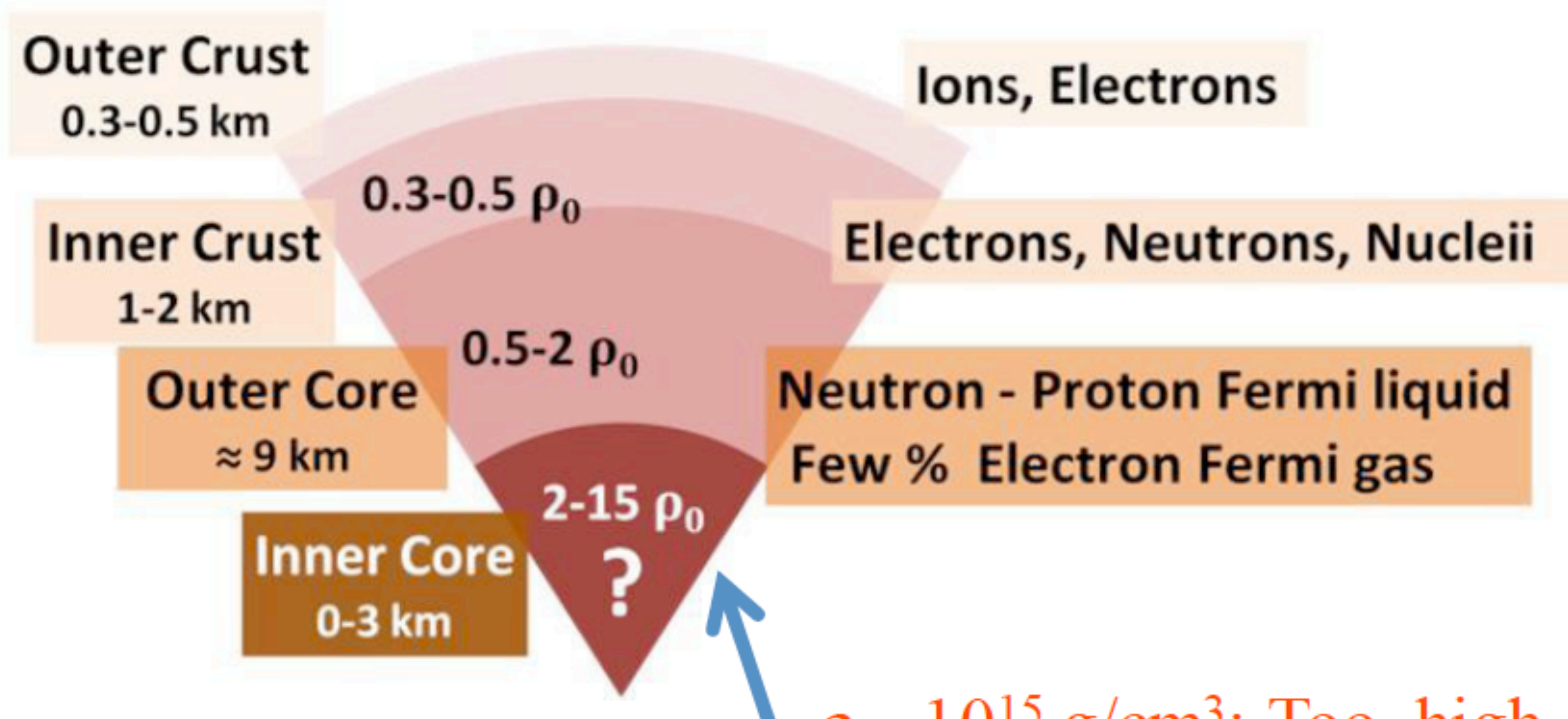

$\rho \sim 10^{15}$ g/cm^3: Too high

$\rho_0 = 2.8 * 10^{14}$ g/cm^3

Components: Neutron + ?????

Radius: 10—15 km ?

Many different possibilities depending on the EOS

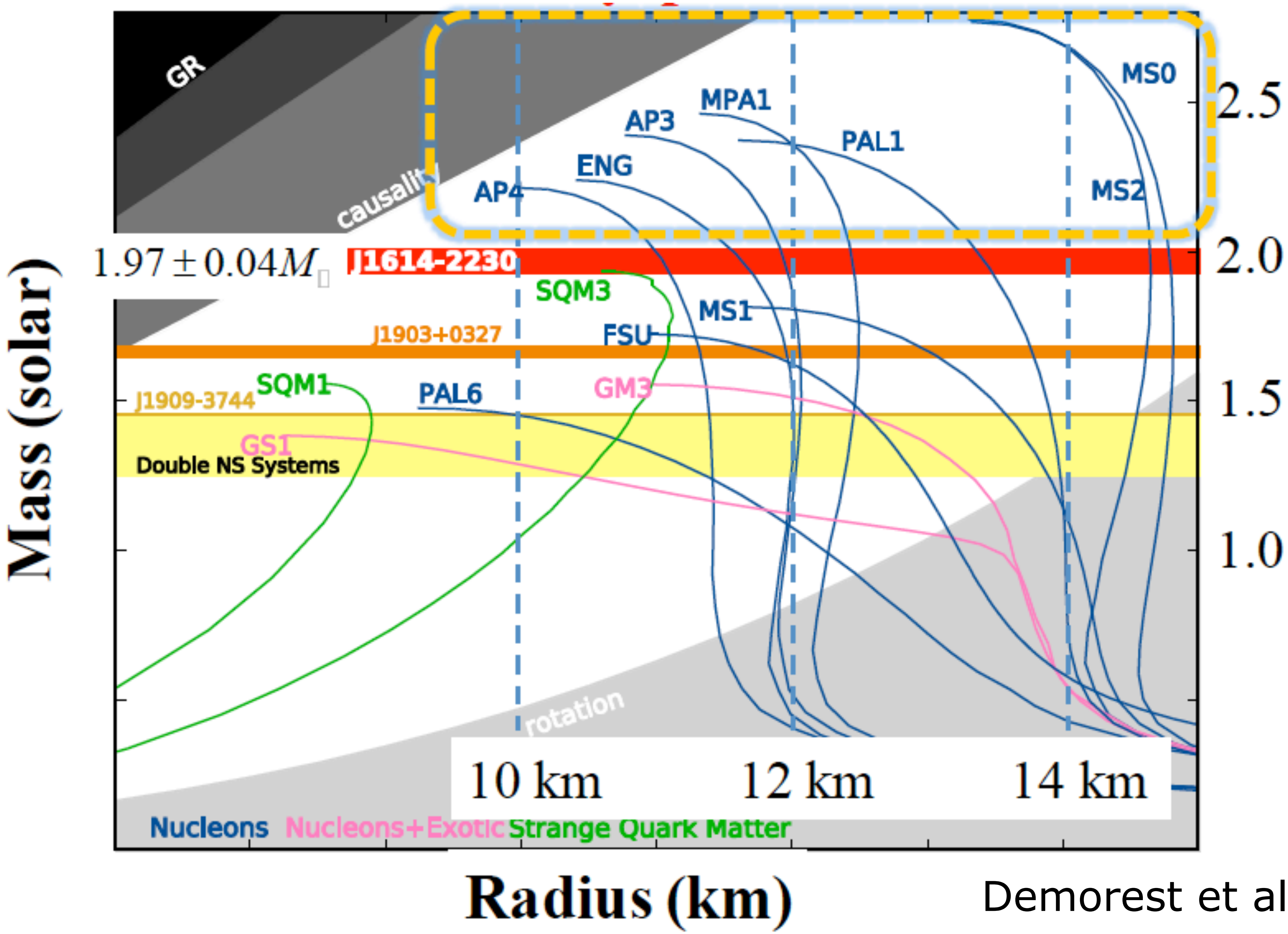

Demorest et al (2010)

GWs in the late inspiral and merger phases could constrain NS EOS.

Many GW templates from Numerical Relativity are necessary

Why study binary neutron star mergers?

Reason #3:

Because their inspiral and merger could be behind one of the most powerful phenomena in the universe: **short Gamma Ray Bursts** (GRBs)

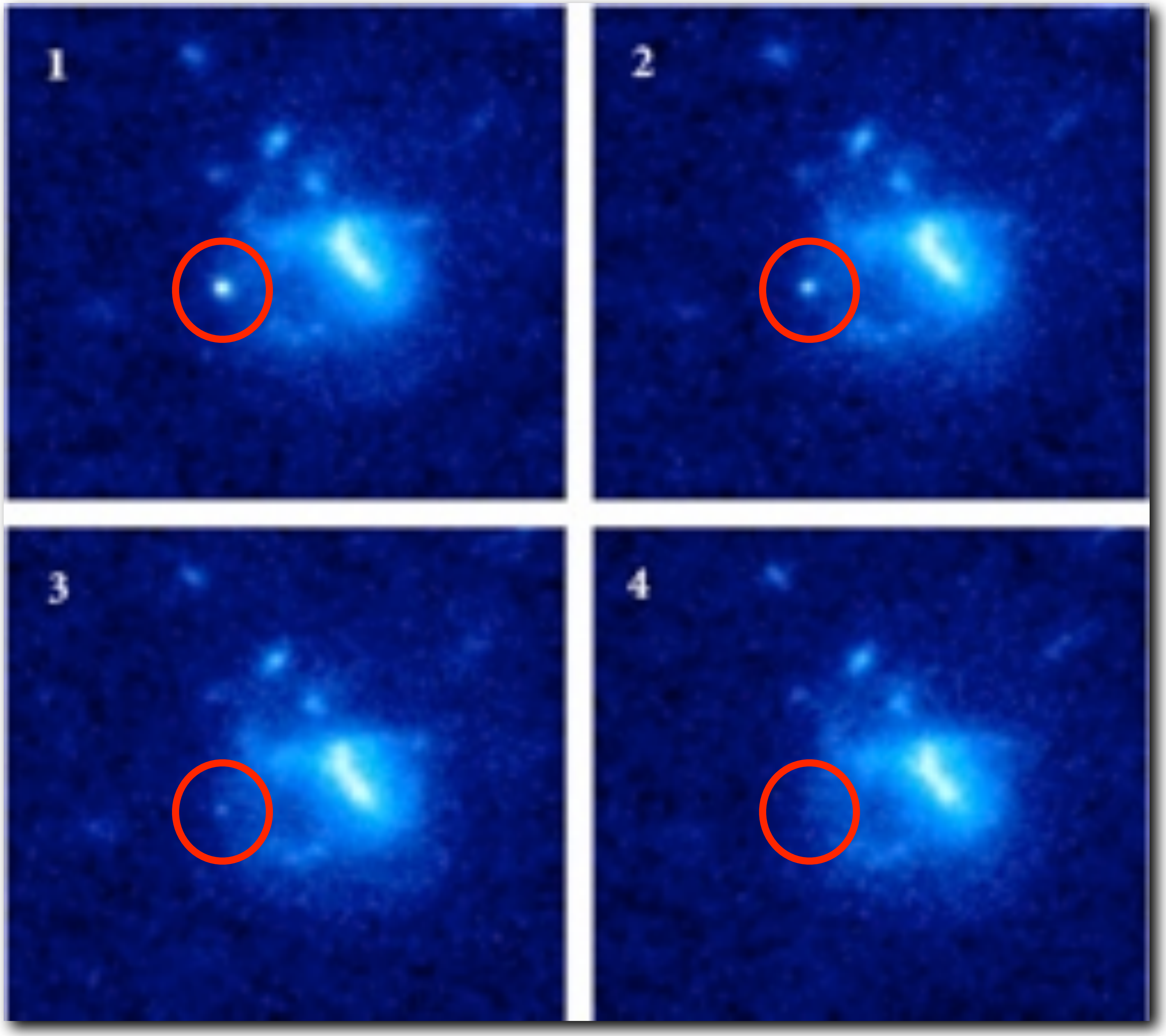

HST images of July 9, 2005 GRB taken 5.6, 9.8, 18.6 & 34.7 days after the burst (Derek Fox, PSU)

Evolution of BNS

Inspiral

- Formation (after two supernovae)
- Evolve as a result of GW emission
- Last 1 hour at $r \sim 1000$ km, $f_{GW} \sim 7$ Hz

Merger starts when $r \sim 30$ km ($f_{GW} \sim 1$ kHz)

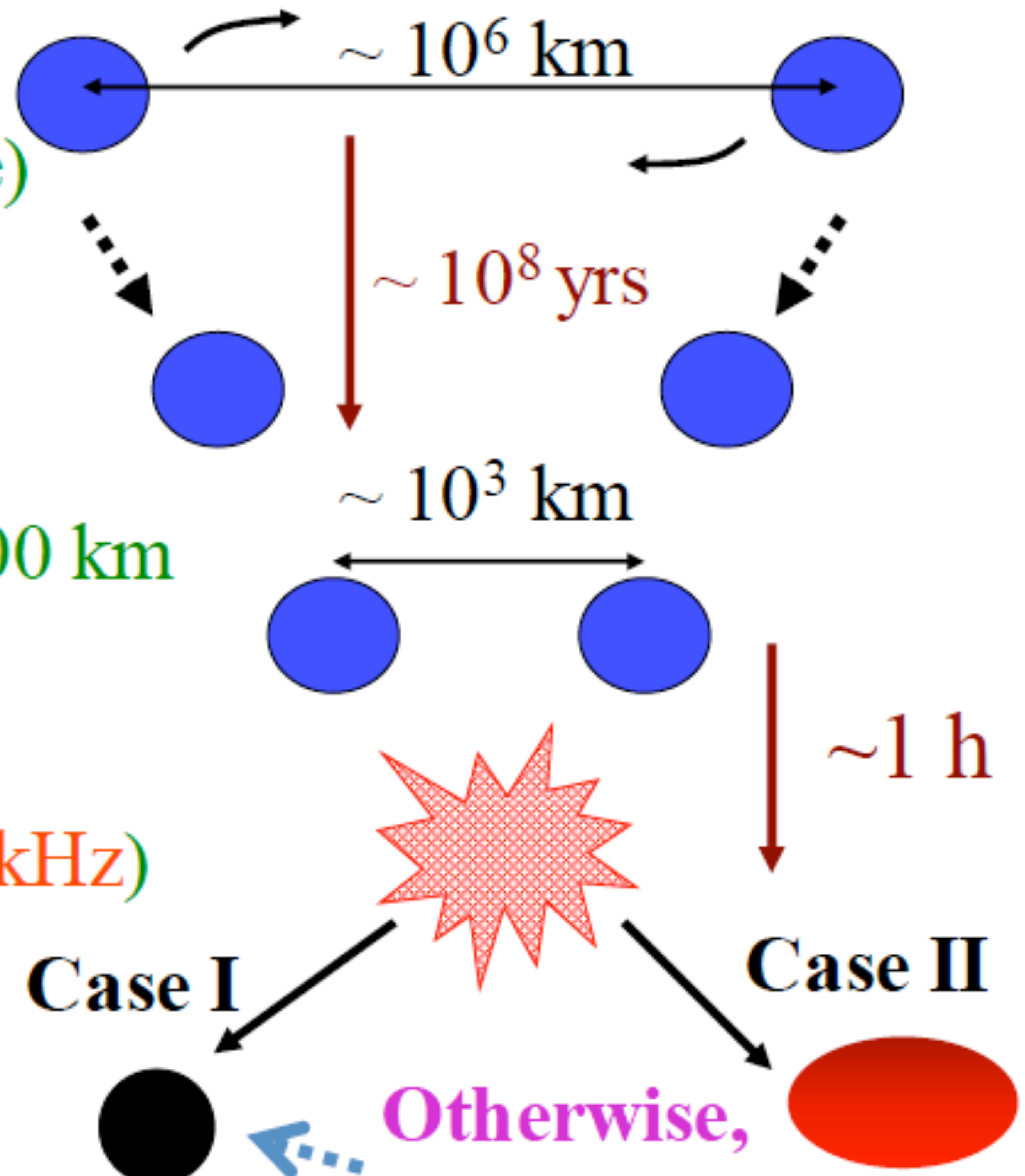

If mass is high enough, a black hole is formed

Otherwise, "hypermasive NS"

Large EOS-dependence

(cf. Shibata)

Galactic compact BNS observed

	PSR	P(day)	e	$M(M_{sun})$	M_1	M_2	T_{GW}
1.	B1913+16	0.323	0.617	2.828	1.387	1.441	2.45
2.	B1534+12	0.421	0.274	2.678	1.333	1.345	22.5
3.	B2127+11C	0.335	0.681	2.71	1.35	1.36	2.2
4.	J0737-3039	0.102	0.088	2.58	1.35	1.24	0.85
5.	J1756-2251	0.32	0.18	2.58	1.31	1.26	1.69
6.	J1906-0746	0.166	0.085	2.62	1.25	1.37	3.0

[according to lowest-order dissipative contribution from GR (2.5PN level); both NSs point masses.]

10^8 yrs

$$\tau_{\rm GW} = \frac{5}{64}\frac{a^4}{\mu M^2} = 2.2\times 10^8 q^{-1}(1+q)^{-1}\left(\frac{a}{R_\odot}\right)^4\left(\frac{M_1}{1.4M_\odot}\right)^{-3}\ {\rm yr}$$

Merger time

6 (GC) NS-NS, which will merge within a Hubble time (13.7 Gyr), have been found.

see Lorimer (2008)

Detection rate by population synthesis

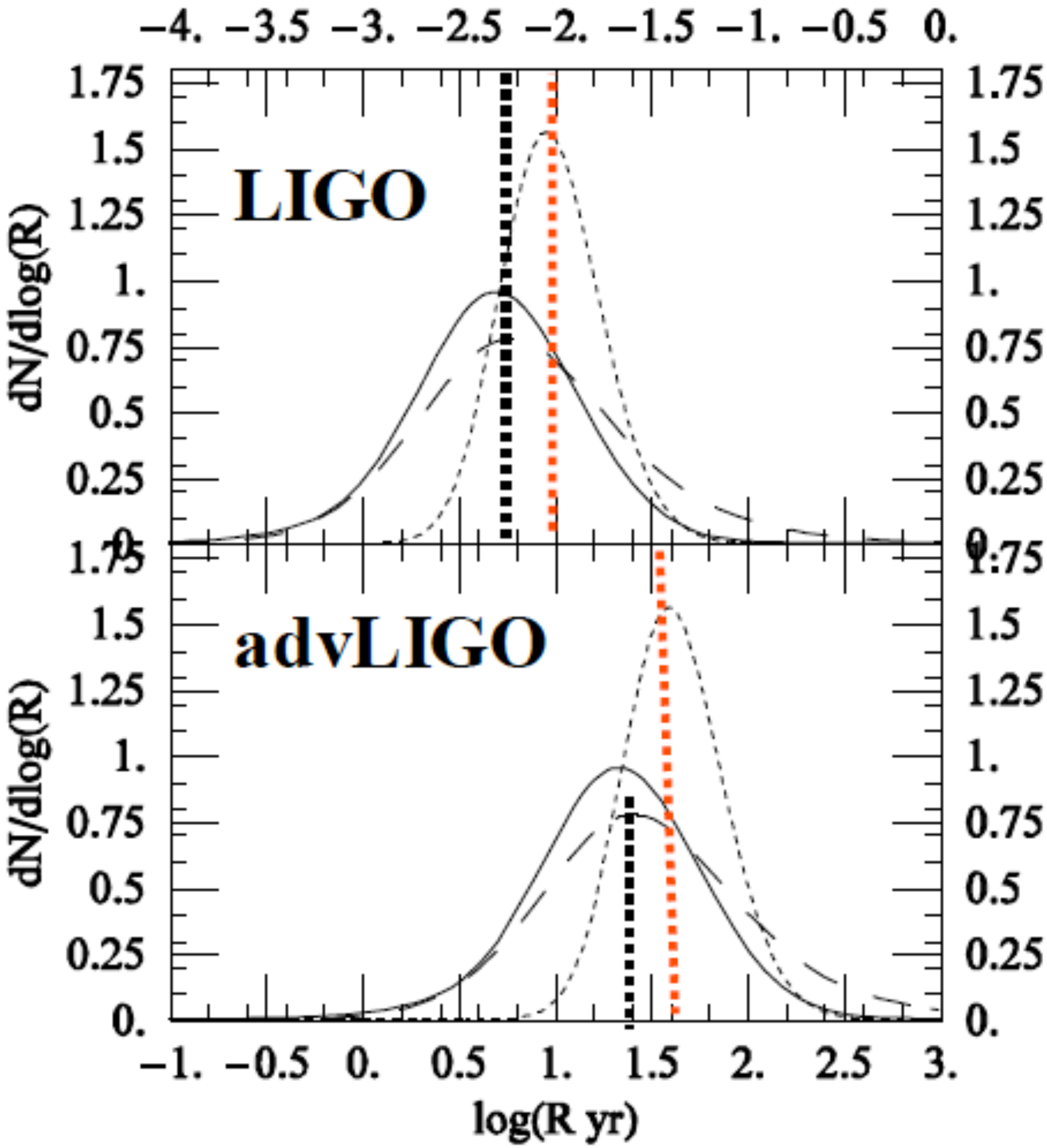

dot： NS/NS

solid： BH/NS

dashed: BH/BH

NS/NS

- 10^{-3}-10^{-1} per year for LIGO
- $10^{0.6}$-$10^{2.6}$ per year for advLIGO

Kalogera et al 2007

A challenging numerical problem

The accurate simulation of a neutron-star–binary merger is among the most challenging tasks in numerical relativity.

These scenarios involve **strong gravitational fields**, matter motion with (ultra) **relativistic speeds**, relativistic **shock waves**, and **strong magnetic fields.**

Numerical difficulties aggravated by intrinsic **multidimensional** character and by the inherent complexities in Einstein's theory of gravity, such as **coordinate degrees of freedom** and the possible formation of **curvature singularities** (black hole formation).

Not surprisingly, early simulations were performed in Newtonian framework (see Faber & Rasio 2012 for a review). Many studies employ Lagrangian particle methods such as SPH; only a few considered (less viscous) high-order finite-volume methods such as PPM (Ruffert & Janka 1998).

Despite difficulties, major progress achieved during <u>last decade</u> in numerical relativity simulations of BNS mergers.

A decade of numerical relativity progress

Drastic **improvements** in simulation front

- **mathematics** (formulation of equations)
- **physics** (nuclear physics EOS, thermal effects, cooling, and MHD)
- **numerical methods** (use of high-resolution methods and adaptive mesh refinement)
- increased **computational resources**

have all allowed to extend scope of early numerical relativity simulations (seminal work by **Shibata and Uryu 2000**).

Increasing attention in recent years by growing number of groups: Kyoto/Tokyo, LSU, AEI, Jena, UIUC, Valencia.

Larger initial separations have recently started being considered and some of the existing simulations have expanded the range spanned by the models well beyond black-hole formation.

Still, most simulations: cold EOS; few include thermal EOS, neutrino effects, and MHD.

Summary of full GR BNS mergers (up to 2012)

	Group	Ref.	NS EOS	Mass ratio	$\mathcal{C}$	notes
Japanese group	KT	[287]	$\Gamma = 2$	1	$0.09 - 0.15$	Co/Ir
	–	[288]	$\Gamma = 2, 2.25$	$0.89 - 1$	$0.1 - 0.17$	
	–	[285]	$\Gamma = 2$	$0.85 - 1$	$0.1 - 0.12$	
	–	[286]	SLy, FPS+Hot	$0.92 - 1$	$0.1 - 0.13$	
	–	[282]	SLy, APR+Hot	$0.64 - 1$	$0.11 - 0.13$	
	–	[332]	$\Gamma = 2$	$0.85 - 1$	$0.14 - 0.16$	BHB
	–	[144]	APR+Hot	$0.8 - 1$	$0.14 - 0.18$	
	–	[145]	APR, SLy, FPS+Hot	$0.8 - 1.0$	$0.16 - 0.2$	
	–	[265]	Shen	1	$0.14 - 0.16$	ν-leak
	–	[134]	PP+hot	1	$0.12 - 0.17$	
	–	[264]	Shen, Hyp	1.0	$0.14 - 0.16$	ν-leak
LSU	HAD	[7]	$\Gamma = 2$	1.0	0.08	GH, non-QE
	–	[6]	$\Gamma = 2$	1.0	0.08	GH, non-QE, MHD
AEI group	Whisky	[17]	$\Gamma = 2$	1.0	$0.14 - 0.18$	
	–	[18]	$\Gamma = 2$	1.0	0.20	
	–	[116]	$\Gamma = 2$	1.0	$0.14 - 0.18$	MHD
	–	[117]	$\Gamma = 2$	1.0	$0.14 - 0.18$	MHD
	–	[240]	$\Gamma = 2$	$0.70 - 1.0$	$0.09 - 0.17$	
	–	[14, 15]	$\Gamma = 2$	1.0	$0.12 - 0.14$	
	–	[241]	$\Gamma = 2$	1.0	0.18	MHD
	UIUC	[172]	$\Gamma = 2$	$0.85 - 1$	$0.14 - 0.18$	MHD
	Jena	[308, 41]	$\Gamma = 2$	1.0	0.14	
	–	[122]	$\Gamma = 2$	1.0	1.4	Eccen.

Faber & Rasio (2012)

Numerical framework for the simulations

It is somehow becoming standardized for most existing codes

Gravitational field eqs

Use conformal and traceless “3+1” formulation of Einstein equations (BSSN)

Gauge: “1+log” slicing for lapse; hyperbolic “Gamma-driver” for shift

Use consistent configurations of irrotational binary NSs in quasi-circular orbit

Use 4th-8th order finite-differencing

Wave-extraction with Weyl scalars and gauge-invariant perturbations

Hydrodynamics/MHD eqs

Riemann-solver-based HRSC TVD methods (HLLE, Roe, Marquina) with high-order cell reconstruction (minmod, PPM)

Method of lines for time integration (high-order conservative RK schemes)

Use excision if needed

Divergence-free magnetic field condition (CT, divergence cleaning)

AMR with moving grids

Basic set of equations to solve
Hydrodynamics

3+1 formulation. Details in Banyuls et al 1997, Font 2008.

$$\boxed{\frac{\partial}{\partial x^\mu}(\sqrt{-g}\rho u^\mu) = 0\,, \qquad \frac{\partial}{\partial x^\mu}(\sqrt{-g}T^{\mu\nu}) = \sqrt{-g}\Gamma^\nu_{\mu\lambda}T^{\mu\lambda}}$$

Hyperbolic system:

$$\frac{1}{\sqrt{-g}}\left(\frac{\partial\sqrt{\gamma}\mathbf{U}}{\partial x^0} + \frac{\partial\sqrt{-g}\mathbf{F}^i}{\partial x^i}\right) = \mathbf{S}$$

$$\begin{aligned}
\mathbf{U} &= (D, S_j, \tau) \\
\mathbf{F}^i &= \left(D\left(v^i - \frac{\beta^i}{\alpha}\right), S_j\left(v^i - \frac{\beta^i}{\alpha}\right) + p\delta^i_j, \tau\left(v^i - \frac{\beta^i}{\alpha}\right) + pv^i\right) \\
\mathbf{S} &= \left(0, T^{\mu\nu}\left(\frac{\partial g_{\nu j}}{\partial x^\mu} - \Gamma^\delta_{\nu\mu}g_{\delta j}\right), \alpha\left(T^{\mu 0}\frac{\partial \ln\alpha}{\partial x^\mu} - T^{\mu\nu}\Gamma^0_{\nu\mu}\right)\right)
\end{aligned}$$

First-order flux-conservative hyperbolic system

Basic set of equations to solve
Magneto-hydrodynamics

Conservation of mass: $\nabla_\mu(\rho u^\mu) = 0$

Conservation of energy and momentum: $\nabla_\mu T^{\mu\nu} = 0$

Maxwell's equations: $\nabla_\mu {}^*F^{\mu\nu} = 0 \quad {}^*F^{\mu\nu} = \frac{1}{W}(u^\mu B^\nu - u^\nu B^\mu)$

- Divergence-free constraint: $\vec{\nabla} \cdot \vec{B} = 0$
- Induction equation: $\frac{1}{\sqrt{\gamma}}\frac{\partial}{\partial t}\left(\sqrt{\gamma}\vec{B}\right) = \vec{\nabla} \times \left[\left(\alpha\vec{v} - \vec{\beta}\right) \times \vec{B}\right]$

Adding all up (Antón et al 2006):
first-order, flux-conservative, hyperbolic system + constraint

$$\boxed{\frac{1}{\sqrt{-g}}\left(\frac{\partial\sqrt{\gamma}\mathbf{U}}{\partial t} + \frac{\partial\sqrt{-g}\mathbf{F}^i}{\partial x^i}\right) = \mathbf{S} \qquad \frac{\partial(\sqrt{\gamma}B^i)}{\partial x^i} = 0}$$

$$D = \rho W \qquad S_j = \rho h^* W^2 v_j - \alpha b_j b^0 \qquad \tau = \rho h^* W^2 - p^* - \alpha^2 (b^0)^2 - D$$

Quite distinct methods used to deal with hyperbolic equations ...

The hyperbolic and conservative nature of the GR(M)HD equations allows to design a solution procedure based on characteristic speeds and fields of the system, translating to relativistic hydro existing tools of CFD.

Godunov-type or **high-resolution shock-capturing (HRSC)** schemes.

Divergence-free constraint not guaranteed to be satisfied numerically when updating the B-field with a HRSC scheme.

Ad-hoc scheme has to be used, e.g. the constrained transport (CT) scheme (Evans & Hawley 1988, Tóth 2000). Main physical implication of divergence constraint: magnetic flux through a closed surface is zero, essential to the CT scheme.

Basic set of equations to solve
Gravitational field equations

From standard (ADM) 3+1 to conformal, traceless BSSN

Details in Alcubierre 2007, Baumgarte & Shapiro 2010

Evolution equations

$$
\begin{aligned}
(\partial_t - \mathcal{L}_\beta)\tilde{\gamma}_{ij} &= -2\alpha\tilde{A}_{ij} \\
(\partial_t - \mathcal{L}_\beta)\phi &= -\frac{1}{6}\alpha K \\
(\partial_t - \mathcal{L}_\beta)K &= -\gamma^{ij}D_iD_j\alpha + \alpha\left[\tilde{A}_{ij}\tilde{A}^{ij} + \frac{1}{3}K^2 + \frac{1}{2}(\rho + S)\right] \\
(\partial_t - \mathcal{L}_\beta)\tilde{A}_{ij} &= e^{-4\phi}\left[-D_iD_j\alpha + \alpha\left(R_{ij} - S_{ij}\right)\right]^{\mathrm{TF}} + \alpha\left(K\tilde{A}_{ij} - 2\tilde{A}_{il}\tilde{A}^l_j\right) \\
(\partial_t - \mathcal{L}_\beta)\tilde{\Gamma}^i &= -2\tilde{A}^{ij}\partial_j\alpha + 2\alpha\left(\tilde{\Gamma}^i_{jk}\tilde{A}^{kj} - \frac{2}{3}\tilde{\gamma}^{ij}\partial_j K - \tilde{\gamma}^{ij}S_j + 6\tilde{A}^{ij}\partial_j\phi\right) \\
&\quad + \partial_j\left(\beta^l\tilde{\partial}_l\gamma^{ij} - 2\tilde{\gamma}^{m(j}\partial_m\beta^{i)} + \frac{2}{3}\tilde{\gamma}^{ij}\partial_l\beta^l\right)
\end{aligned}
$$

Constraint equations

$$
\begin{aligned}
R + K^2 - K^{ij}K_{ij} &= 16\pi\rho \\
\nabla_i\left(K^{ij} - \gamma^{ij}K\right) &= 8\pi S^j
\end{aligned}
$$

Cauchy problem (IVP):

- Constraint-satisfying ID $\tilde{\gamma}_{ij},\ \phi,\ K,\ \tilde{A}_{ij},\ \tilde{\Gamma}^i$
- Freely specifiable coordinates $\alpha\ \ \beta^i$
- Evolve ID

Gravitational wave extraction in (3+1) NR

First approach: perturbations on a Schwarzschild background expanding spatial metric into a tensor basis of Regge-Wheeler harmonics. Allows for extracting gauge-invariant wavefunctions given spherical surfaces of constant coordinate radius.

Second approach: projection of the Weyl tensor onto components of a null tetrad. At a sufficiently large distance from the source and in a Newman-Penrose tetrad frame, the gravitational waves in the two polarizations can be written in terms of the Weyl scalar.

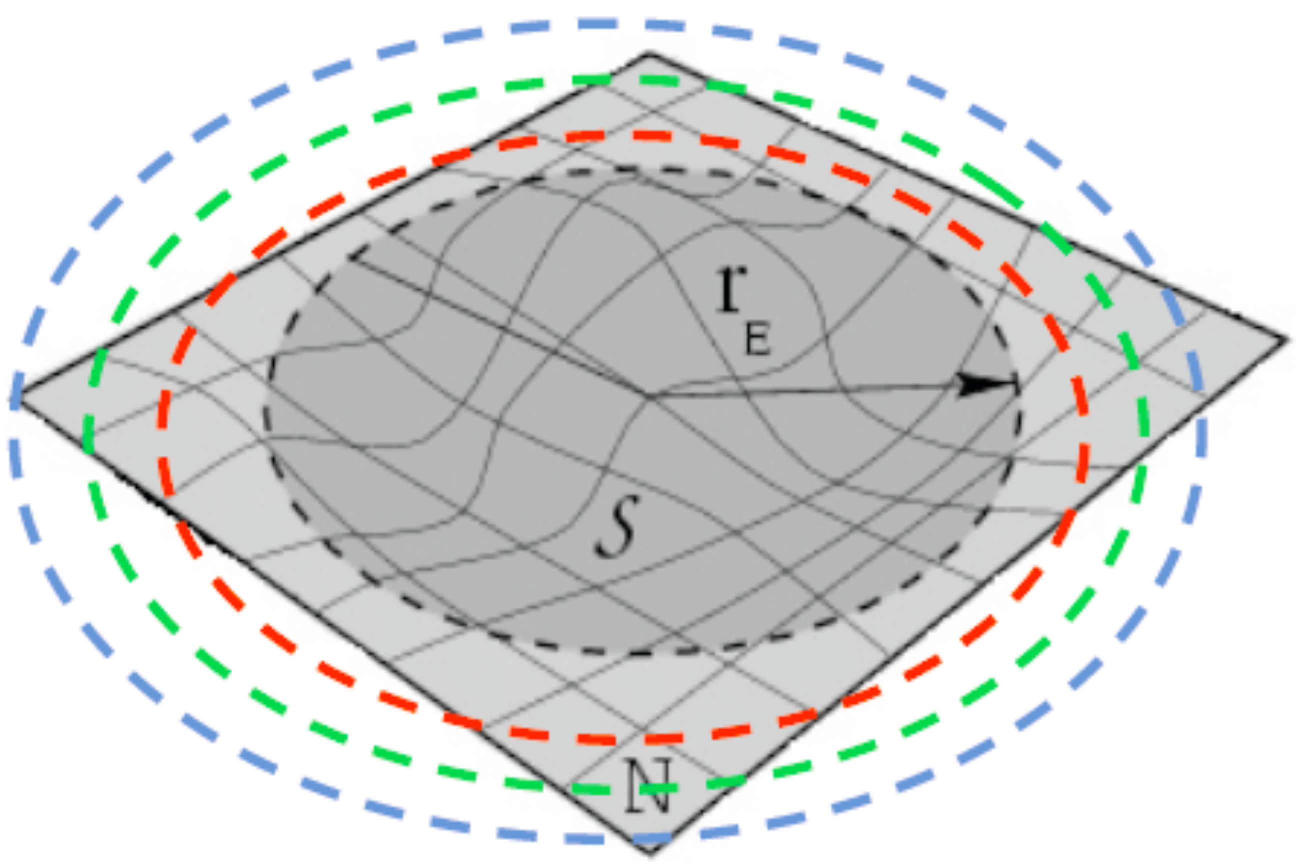

In both approaches observers are located at various positions from the source (nested spheres), where Weyl scalars are computed or where the metric is decomposed in tensor spherical harmonics to compute gauge invariant perturbations of a Schwarzschild black hole.

Shibata's massive body of work on BNS

Most dedicated study of BNS mergers in full general relativity performed by Shibata and coworkers (Kyoto/Tokyo)

Shibata **1999**, 2005 Shibata & Uryu **2000**, 2002 Shibata, Taniguchi & Uryu 2005 Shibata & Taniguchi 2006	Preparatory work Simple EOS
... Hotokezaka, Kyutoku, Okawa, Shibata, Kiuchi 2011 Sekiguchi, Kiuchi, Kyutoku, Shibata 2011 Kiuchi, Sekiguchi, Kyutoku, Shibata, 2012	Mycrophysical EOS GRBs Gravitational waves

- self-consistent initial data for irrotational and corotational binaries
- long-term evolutions: from ISCO up to formation and ringdown of final collapsed object (either a BH or a hypermassive neutron star)
- equal and unequal mass ratio
- apparent horizon finder
- microphysical (thermal) EOS and neutrino cooling (leakage)
- gravitational waveform extraction from the collisions
- state-of-the-art numerical methodology

Main (initial, ideal fluid EOS) results

Final outcome of merger depends significantly on **initial compactness** of NSs before plunge, i.e. on the stiffness of the (ideal fluid) EOS

- If total mass of the system is 1.3–1.7 times larger than maximum rest mass of a spherical star in isolation, end product is a **black hole**.
- Otherwise, a marginally-stable **hypermassive neutron star** forms, supported against self-gravity by rapid differential rotation.

The HMNS will eventually collapse to a black hole once sufficient angular momentum is dissipated via neutrino emission and/or gravitational radiation.

Ultimate outcome of BNS mergers is a black hole + torus system (the more the NS mass ratio departs from unity the larger the disk mass).

Different outcome of the merger imprinted in the gravitational waveforms, as first noted by Shibata & Uryu 2002.

Future detection of GWs from BNS mergers could help constrain the maximum allowed mass of NSs along with the composition of NS matter.

Recently scrutinized in simulations performed by the Kyoto group, in which new ingredients have been incorporated in the modelling (nucleonic and hyperonic finite-temperature EOS and neutrino cooling).

NS/NS: relativistic simulations with realistic EOS

(Shibata, Taniguchi & Uryu, PRD 71, 084021 (2005))

Case 1.30M_{sun} - 1.30M_{sun}

Formation of a hypermassive neutron star

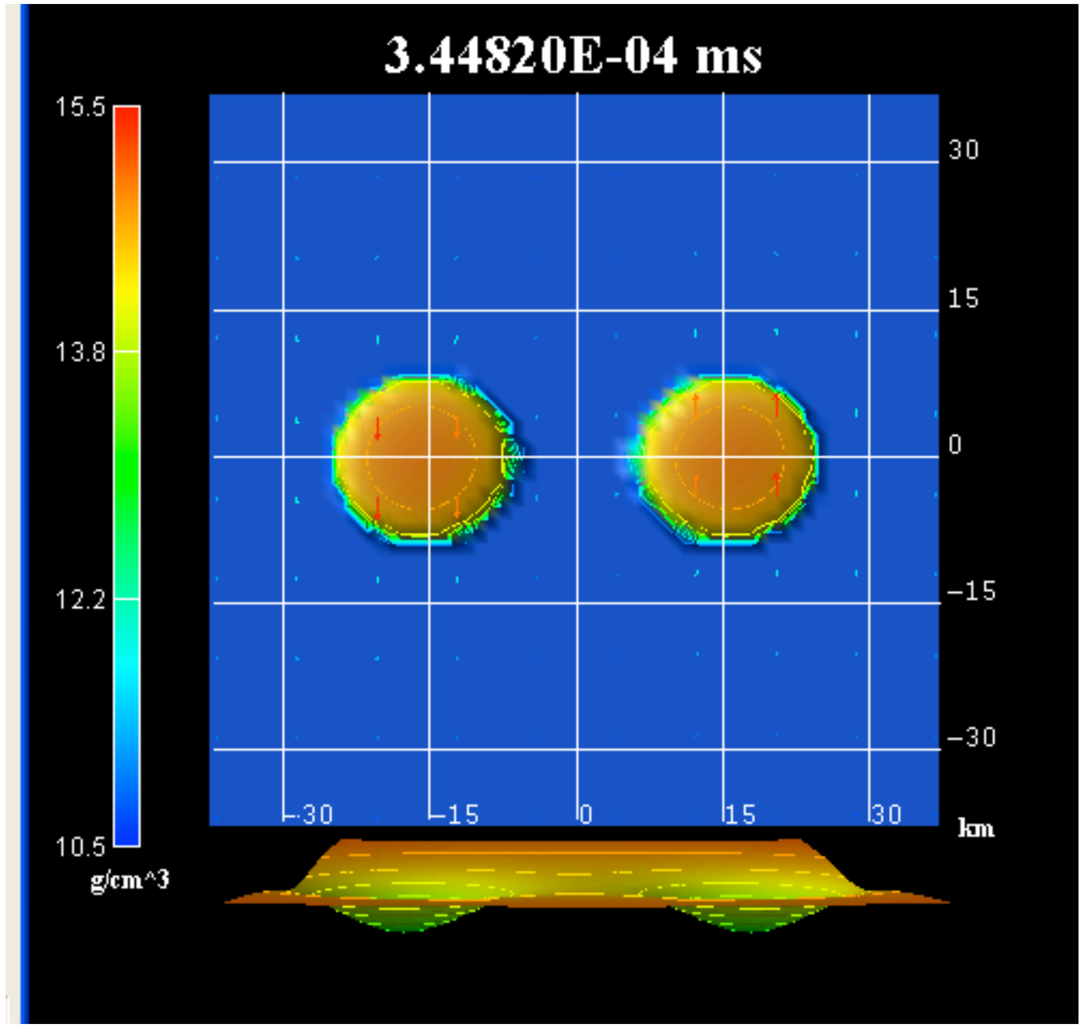

Case 1.35M_{sun} - 1.35M_{sun}

Delayed formation of a rotating black hole

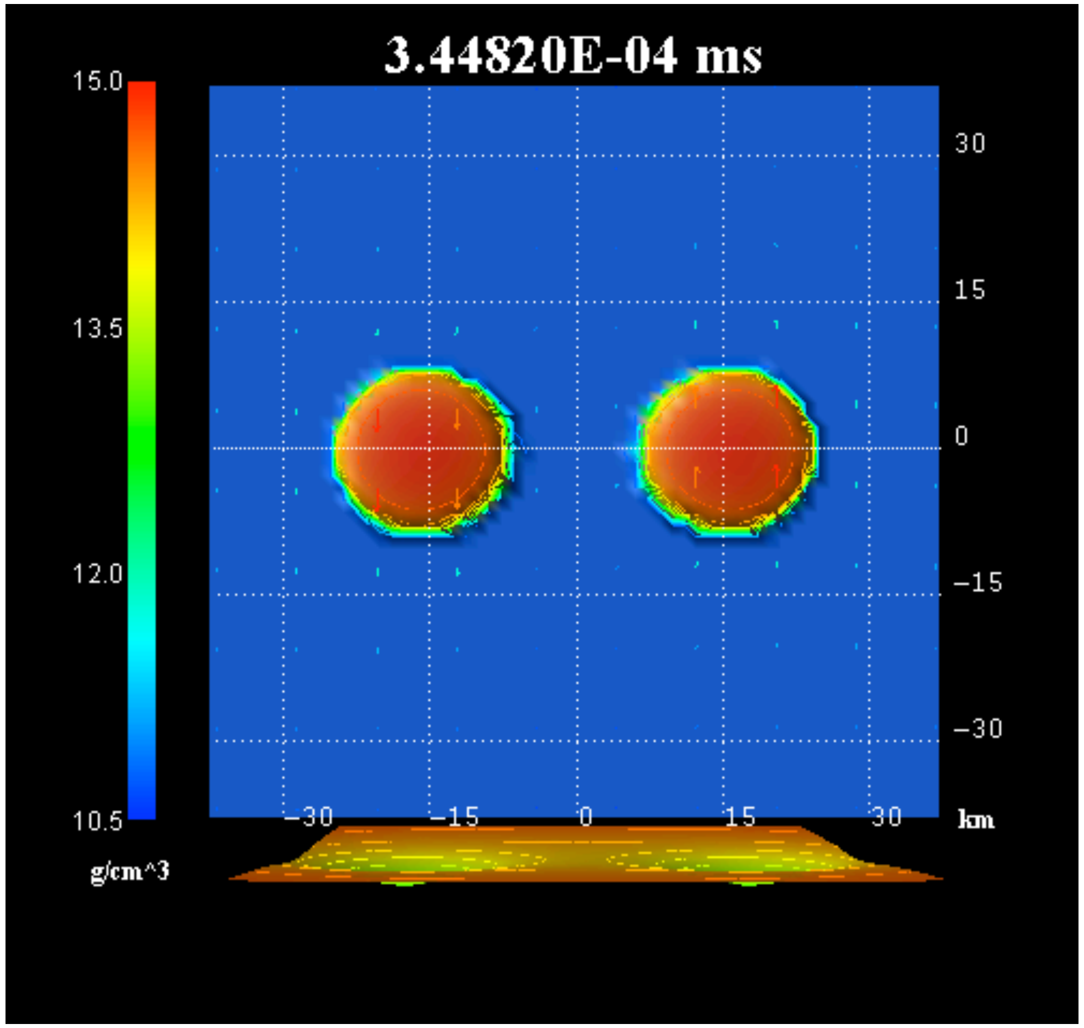

The gravitational waveform allows to unveil the final outcome: neutron star or black hole.

BNS merger → HMNS → BH+torus

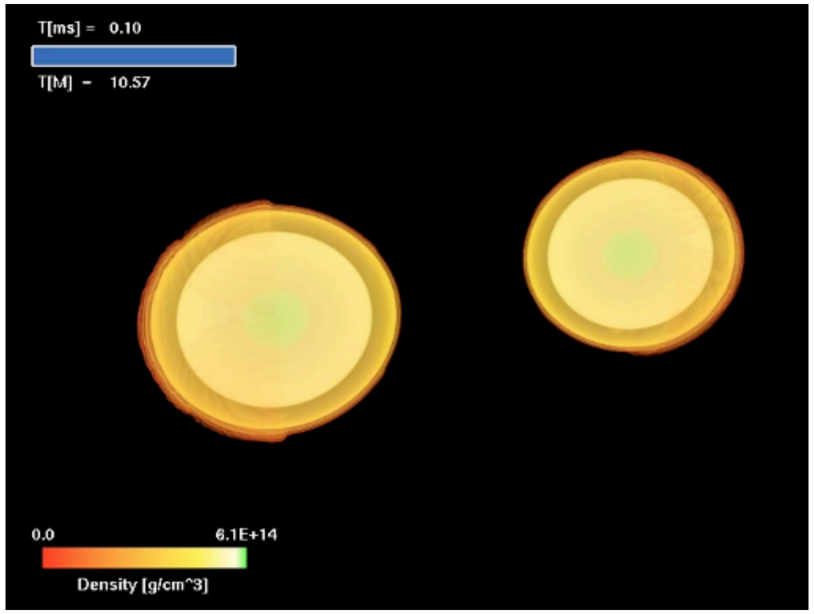

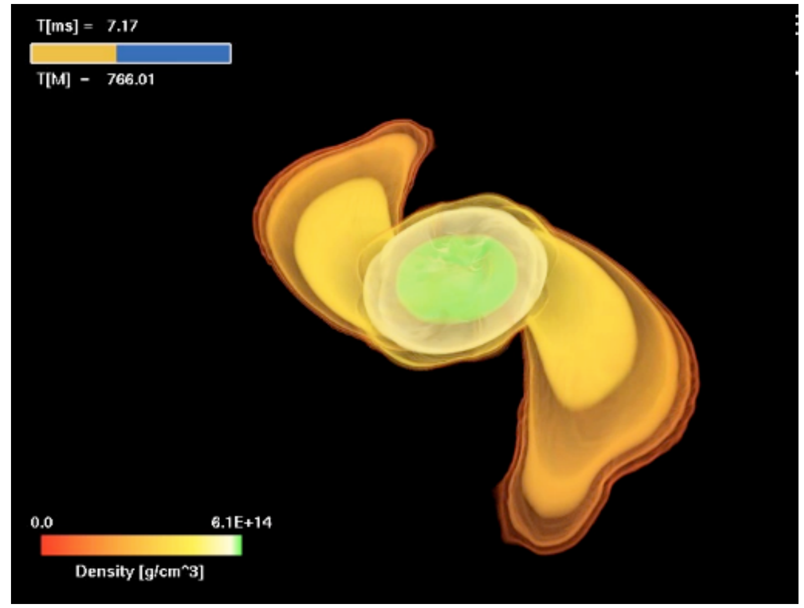

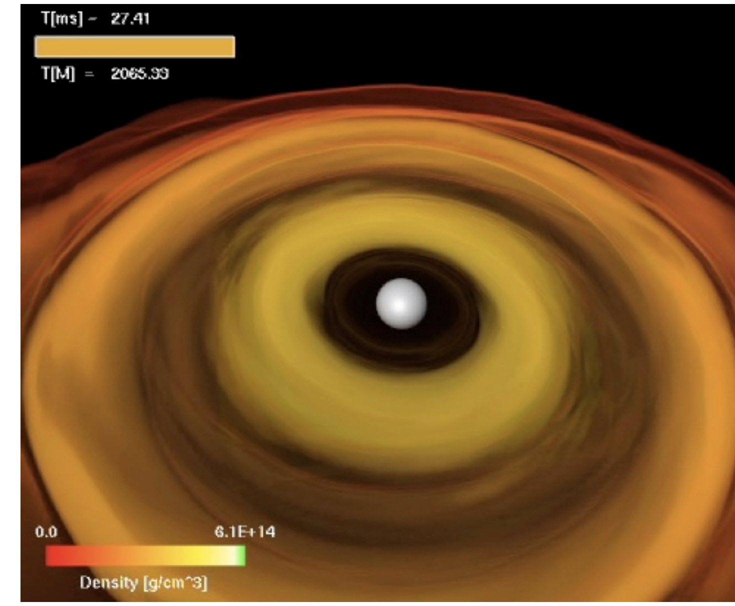

Credit: AEI

Variations on this **general trend** are produced by:

- differences in the mass for the same EOS:

a binary with smaller mass will produce a HMNS which is further away from the stability threshold and will collapse at a later time

- differences in the EOS for the same mass:

a binary with an EOS allowing for a larger thermal internal energy (ie hotter after merger) will have an increased pressure support and will collapse at a later time

Equal-mass BNS merger

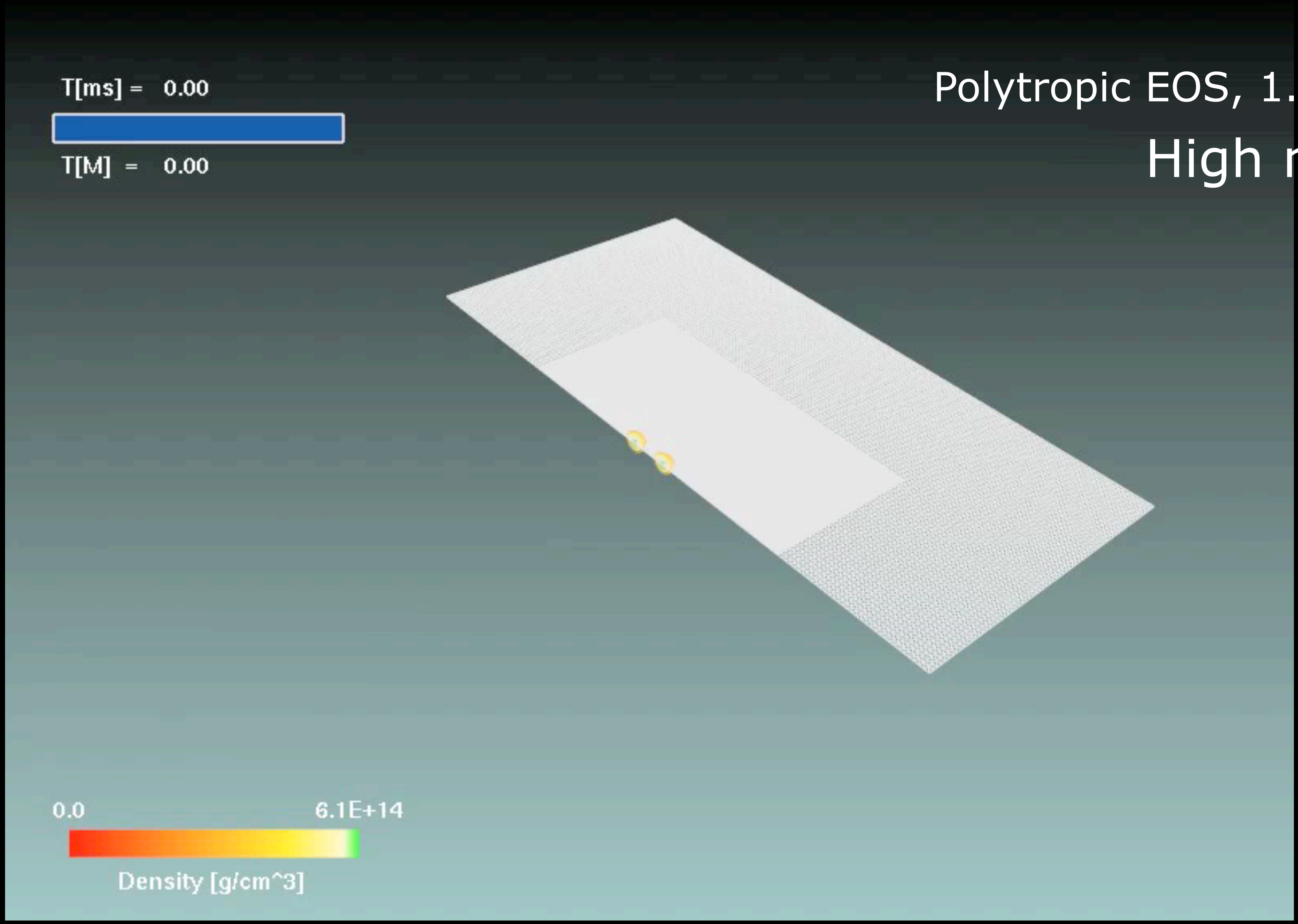

A hot, low-density torus is produced orbiting around the BH.
This is what is expected in short GRBs.

(Baiotti et al 2008)

Polytropic EOS, 1.4 M_{sun}

Low mass

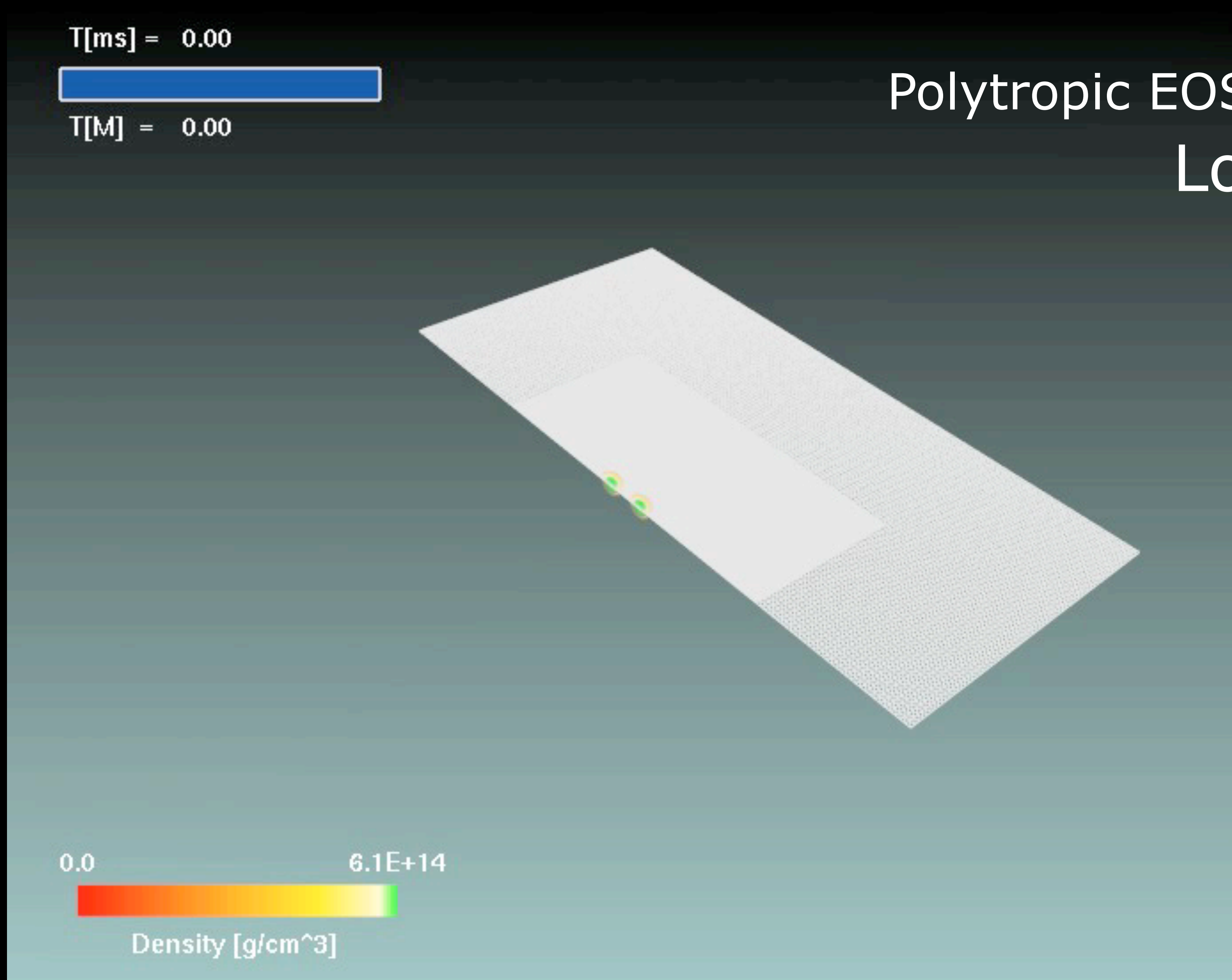

The HMNS is far from the instability threshold and survives for a longer time while losing energy and angular momentum.

After ~ 25 ms the HMNS has lost sufficient angular momentum and will collapse to a BH.

(Baiotti et al 2008)

Matter dynamics: effects of the total mass

high-mass binary

low-mass binary

(Baiotti et al 2008)

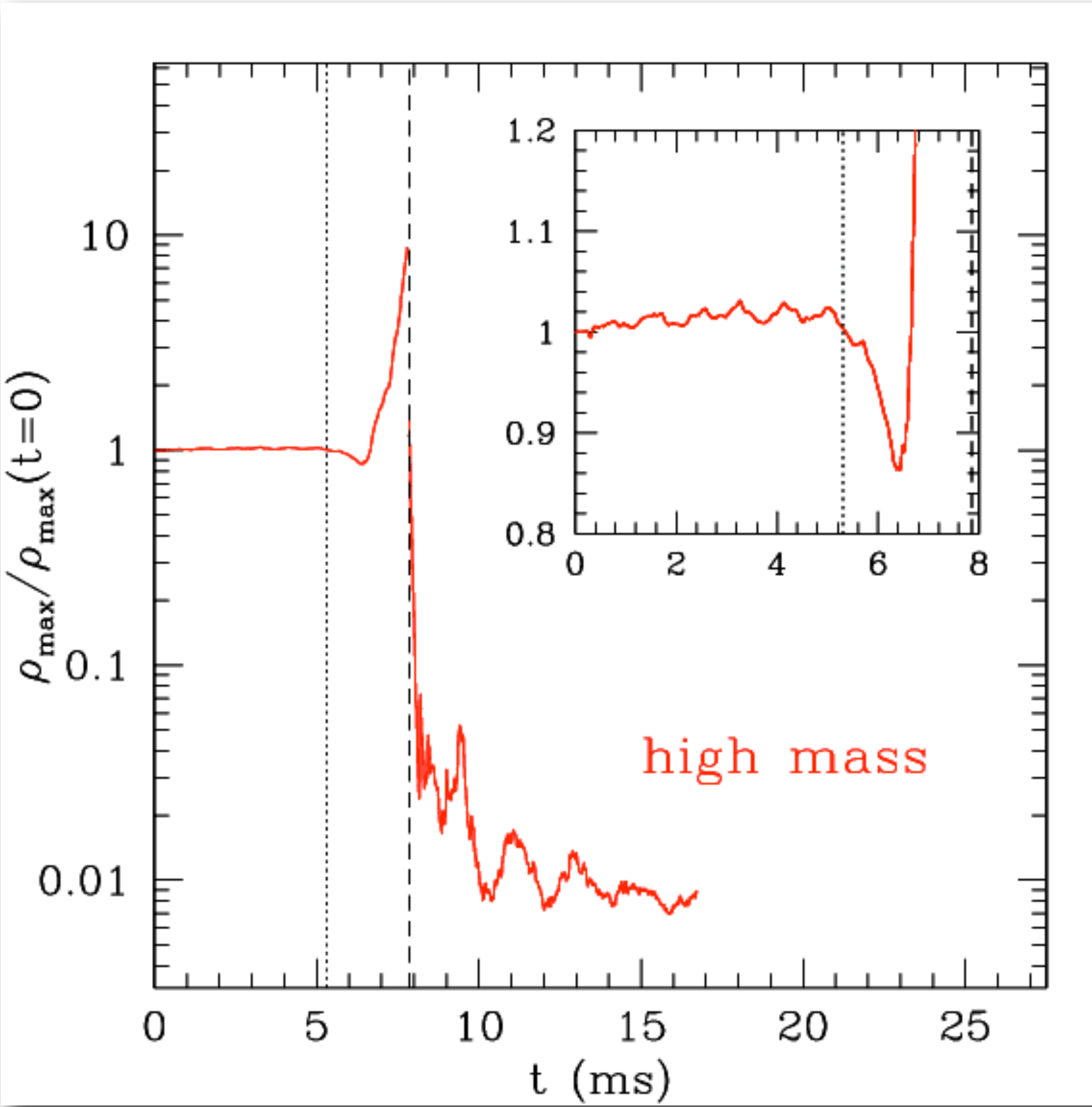

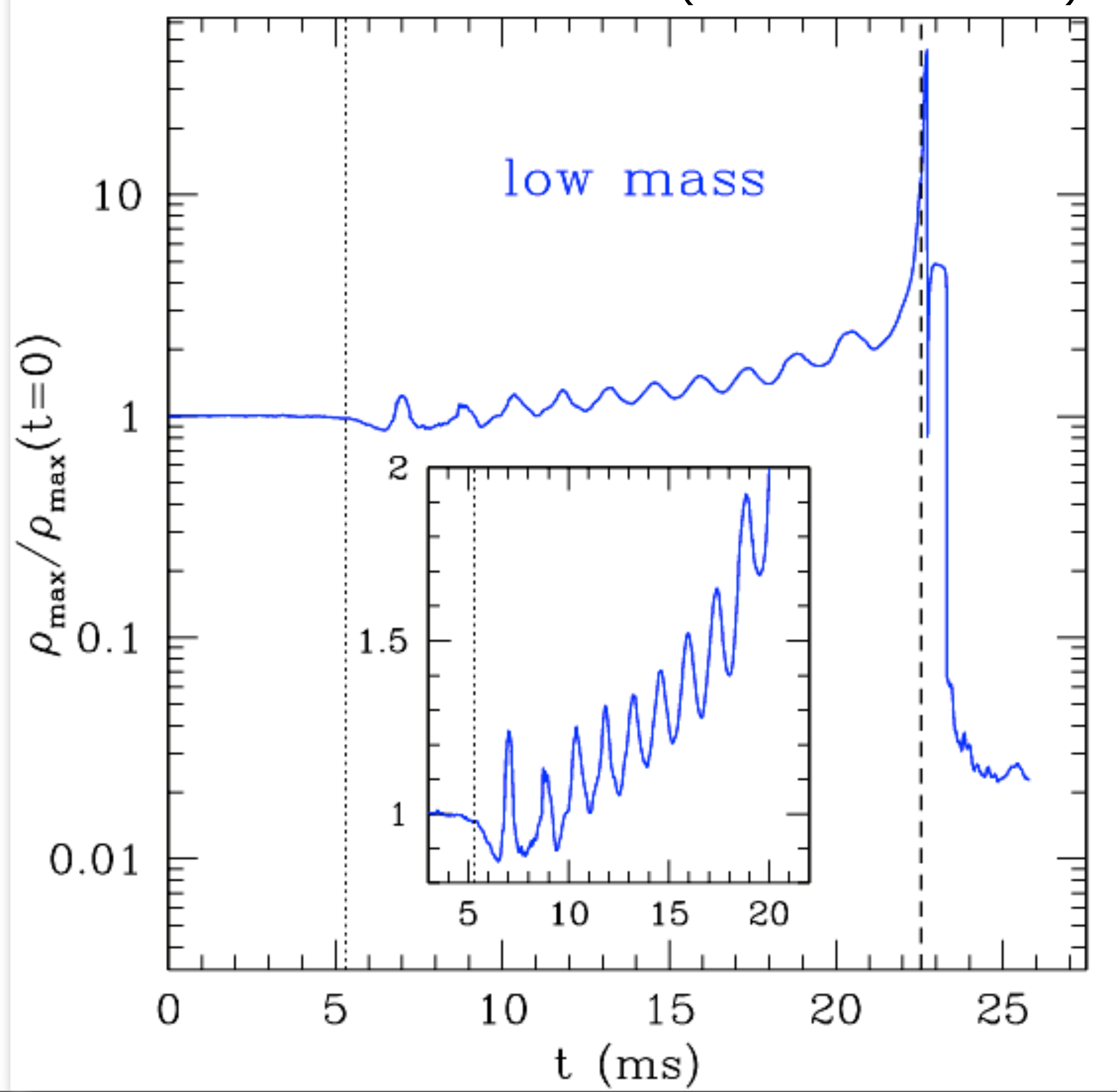

soon after the merger the torus is formed and undergoes oscillations

long after the merger a BH is formed surrounded by a torus

Gravitational radiation from *the* merger

Dynamics

Signal amplitude

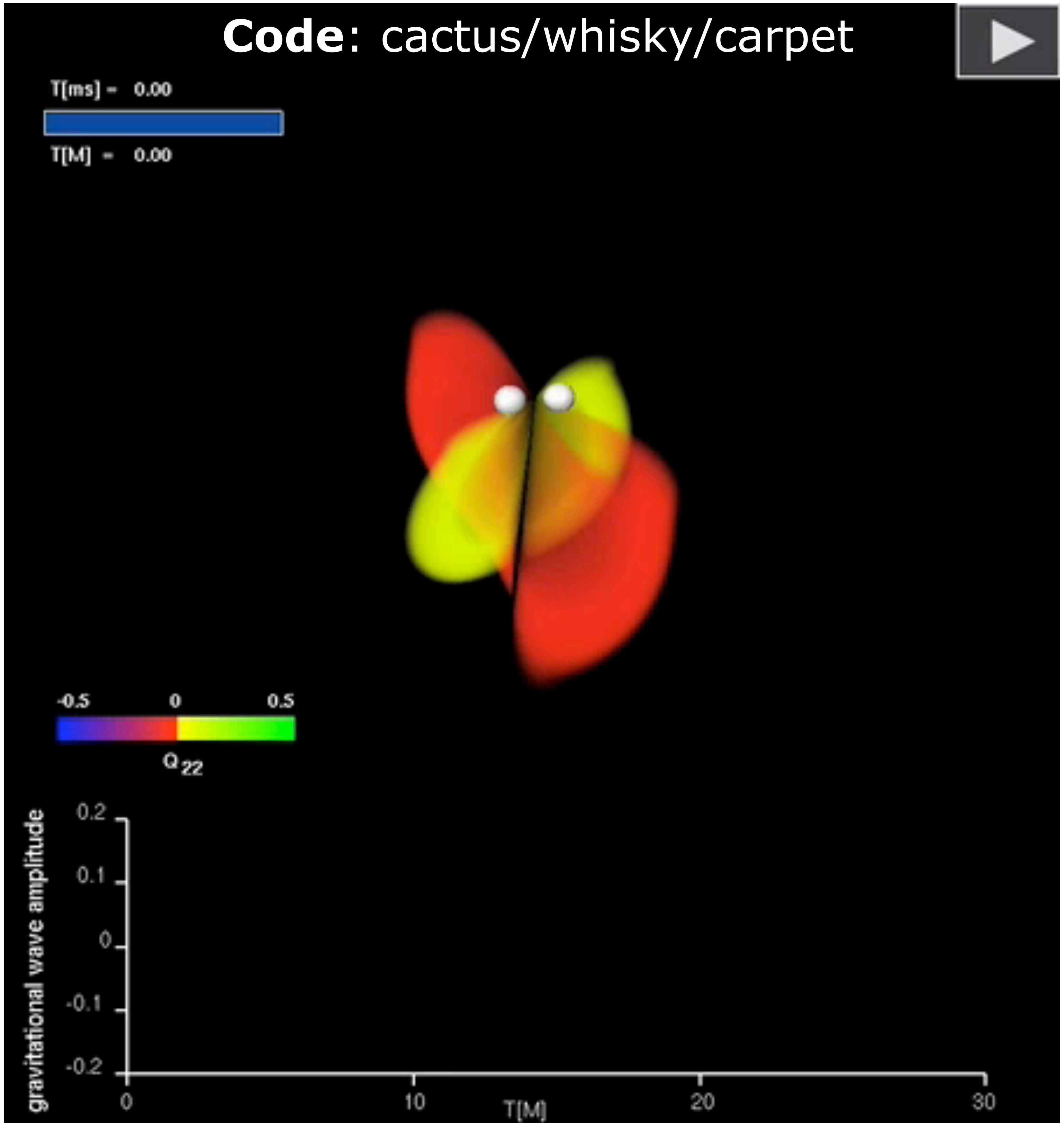

(AEI)

Waveforms: strong dependence on total mass

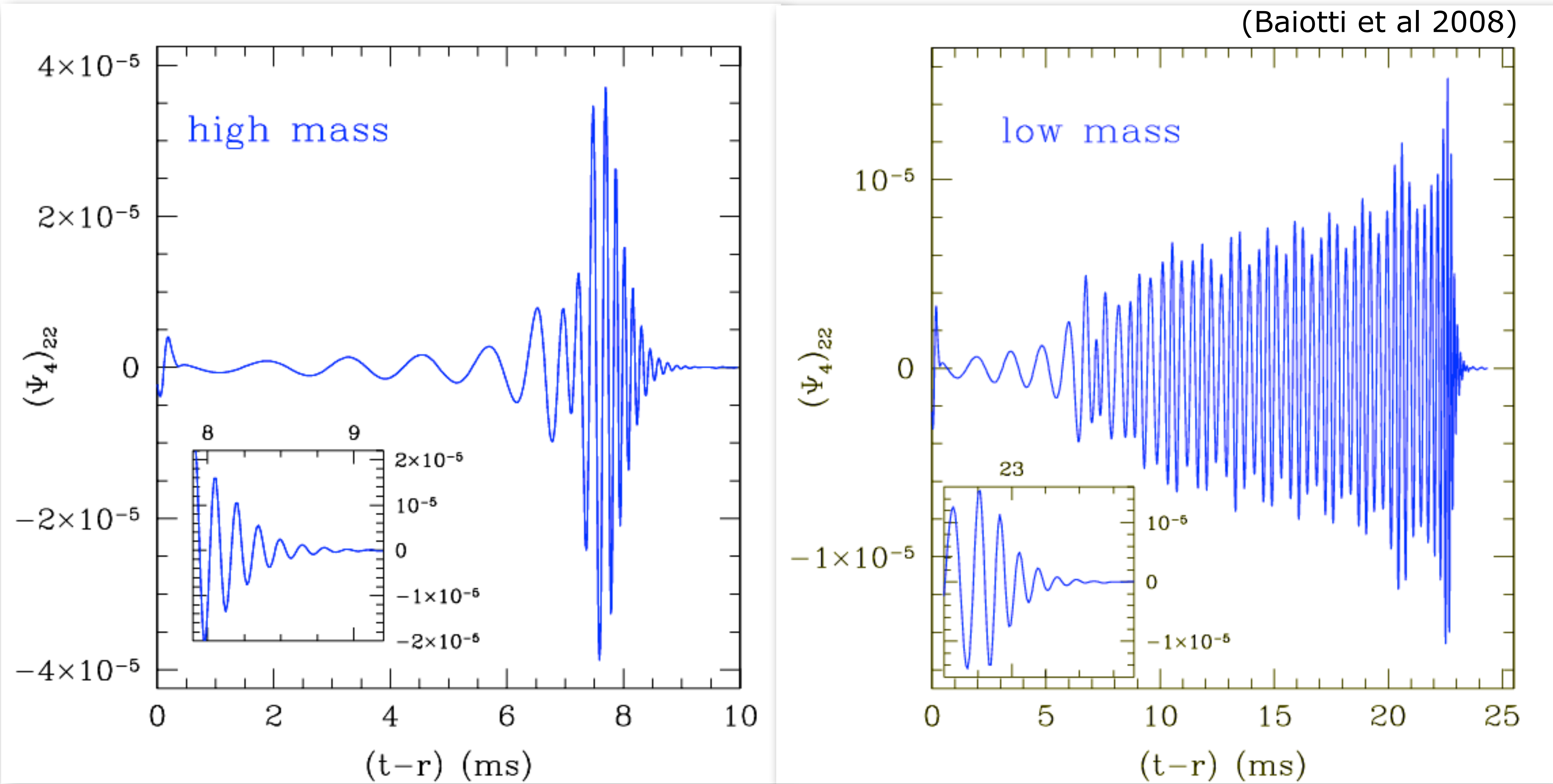

(Baiotti et al 2008)

Small variations in the total mass of the initial models yield important differences in the gravitational waveforms

Imprint of the EOS: ideal fluid vs polytropic

(Baiotti et al 2008)

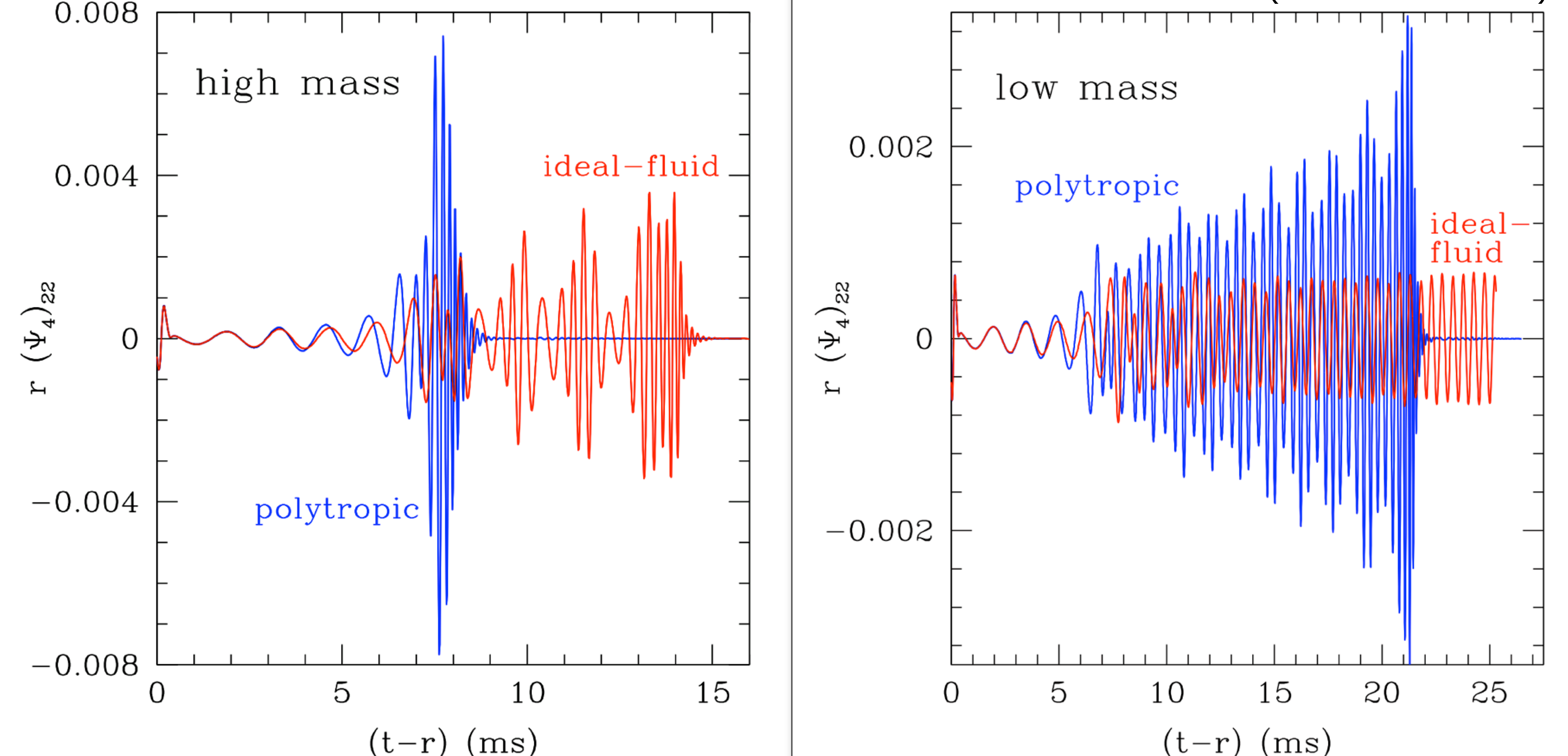

After the merger a BH is produced over a timescale comparable with the dynamical one

After the merger a BH is produced over a timescale larger or much larger than the dynamical one

Increasing realism of simulations thermal conditions of BNSs

Late inspiral phase: neutron stars are **cold.**
Neutron stars with age > 10^7 years have undergone long-term cooling by neutrinos and photons.

$$\mathrm{T} < 10^5\,\mathrm{K} \sim 10\,\mathrm{eV} \ll E_\mathrm{F} \sim 100\,\mathrm{MeV}$$

Hence, neutron stars can be modelled by cold EOS.
Problem: such EOS is still unknown; need for a systematic survey.

Merger phase: neutron stars are **hot.** Shock heating increases temperature to about $\mathrm{kT} \sim 0.1 - 0.2\,E_\mathrm{F} \sim 10\,\mathrm{MeV}$

New effects likely to play important dynamical role: finite temperature effects, lepton fraction, neutrino thermal pressure, neutrino cooling.
Neutron stars modelled by thermal EOS.
Problem: systematic survey as well; few EOS available, more needed.

Dependence on the nuclear EOS

$$P(\rho,\varepsilon) = P_{\rm cold}(\rho) + P_{\rm th}(\rho,\varepsilon)$$

Piecewise-polytropic EOS for the cold part (Read et al 2009)

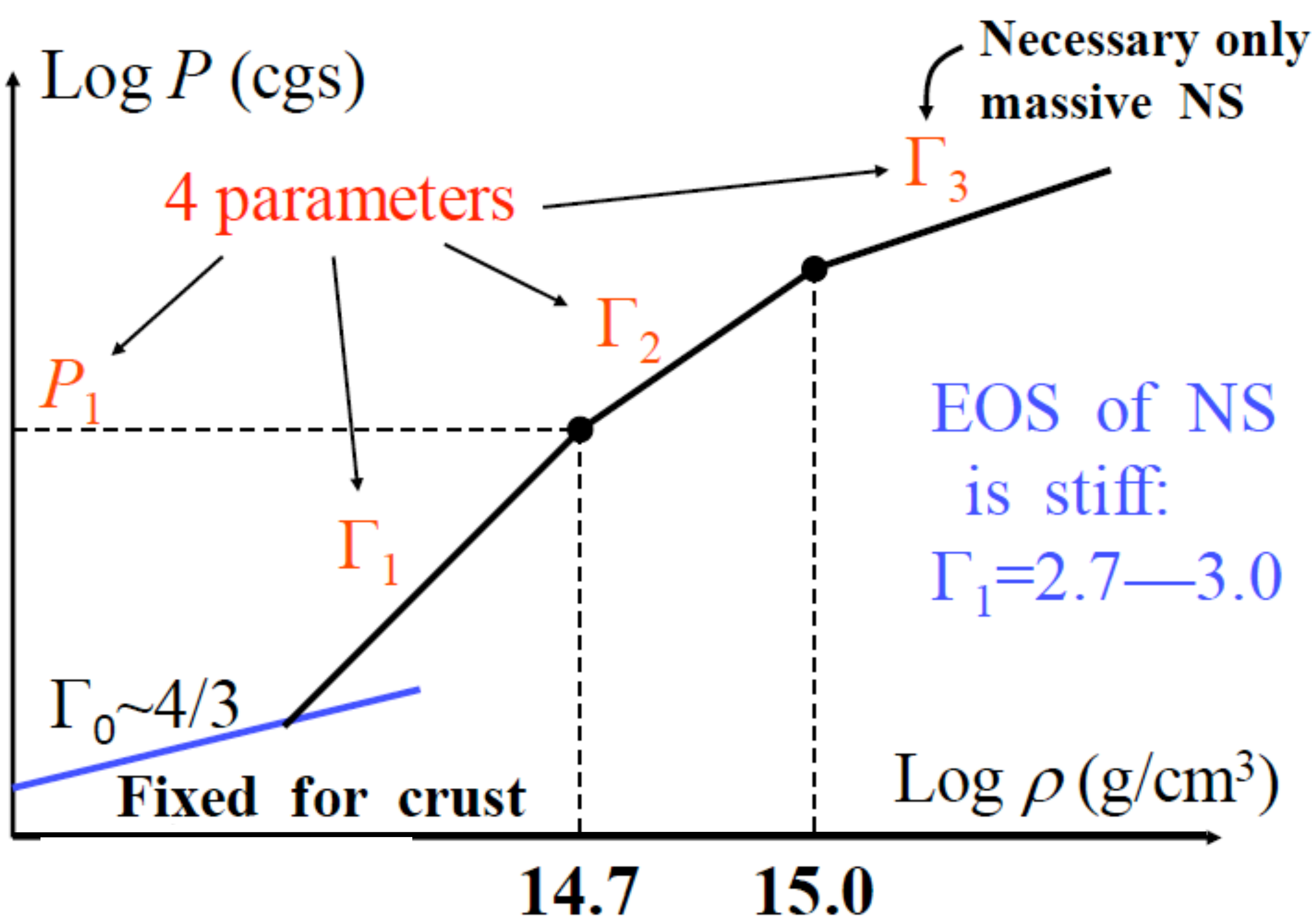

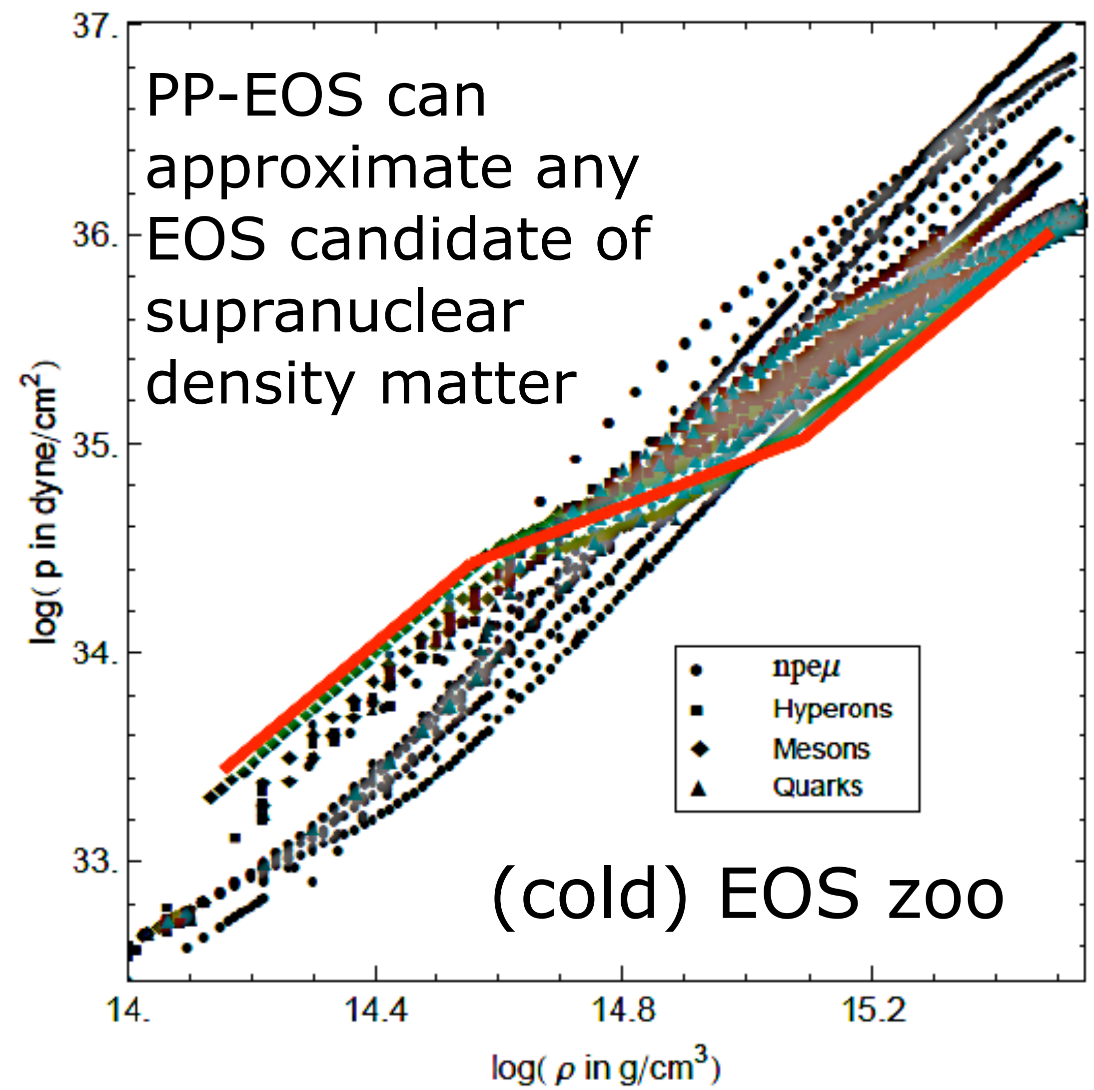

Thermal part of the pressure (shock heating) for hot, merged NS (T~10MeV) given by

$$P_{\rm th} = (\Gamma_{\rm th}-1)(\varepsilon-\varepsilon_{\rm cold})\rho, \quad \Gamma_{\rm th} = 1.357-1.8$$

Type of final remnant depending on the nuclear EOS

Hotokezaka et al (2011)

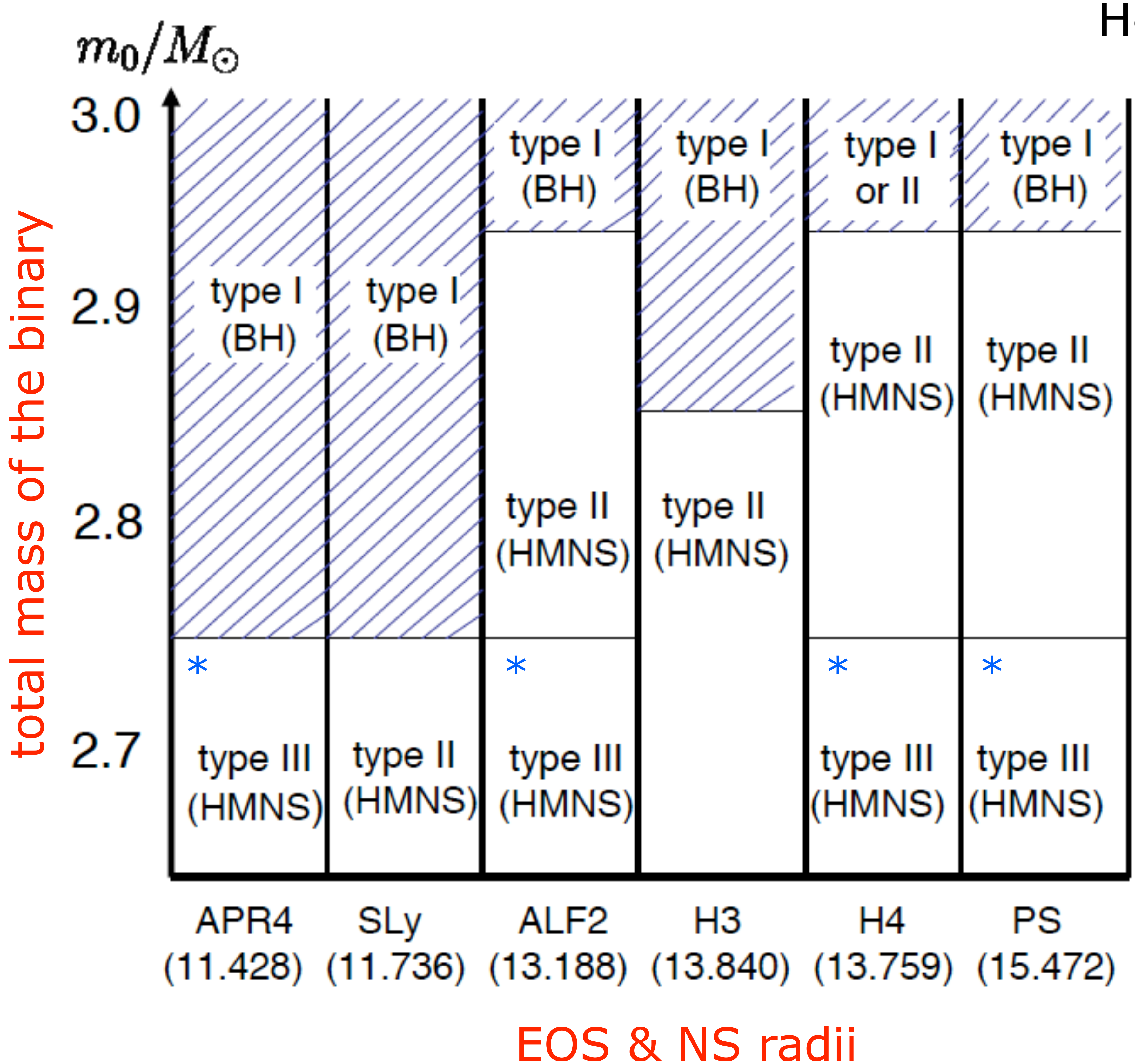

Type I: prompt collapse to BH

Type II: short-lived HMNS (<5 ms)

Type III: long-lived HMNS (>5 ms)

* EOS with M_{max}>2M_{sun}

Demorest et al (2010): discovery of NS with $M=1.97\pm0.04\ M_{sun}$

GW emission depending on the nuclear EOS

Qualitative form of high-frequency components of GW signal primarily determined by type of remnant formed.

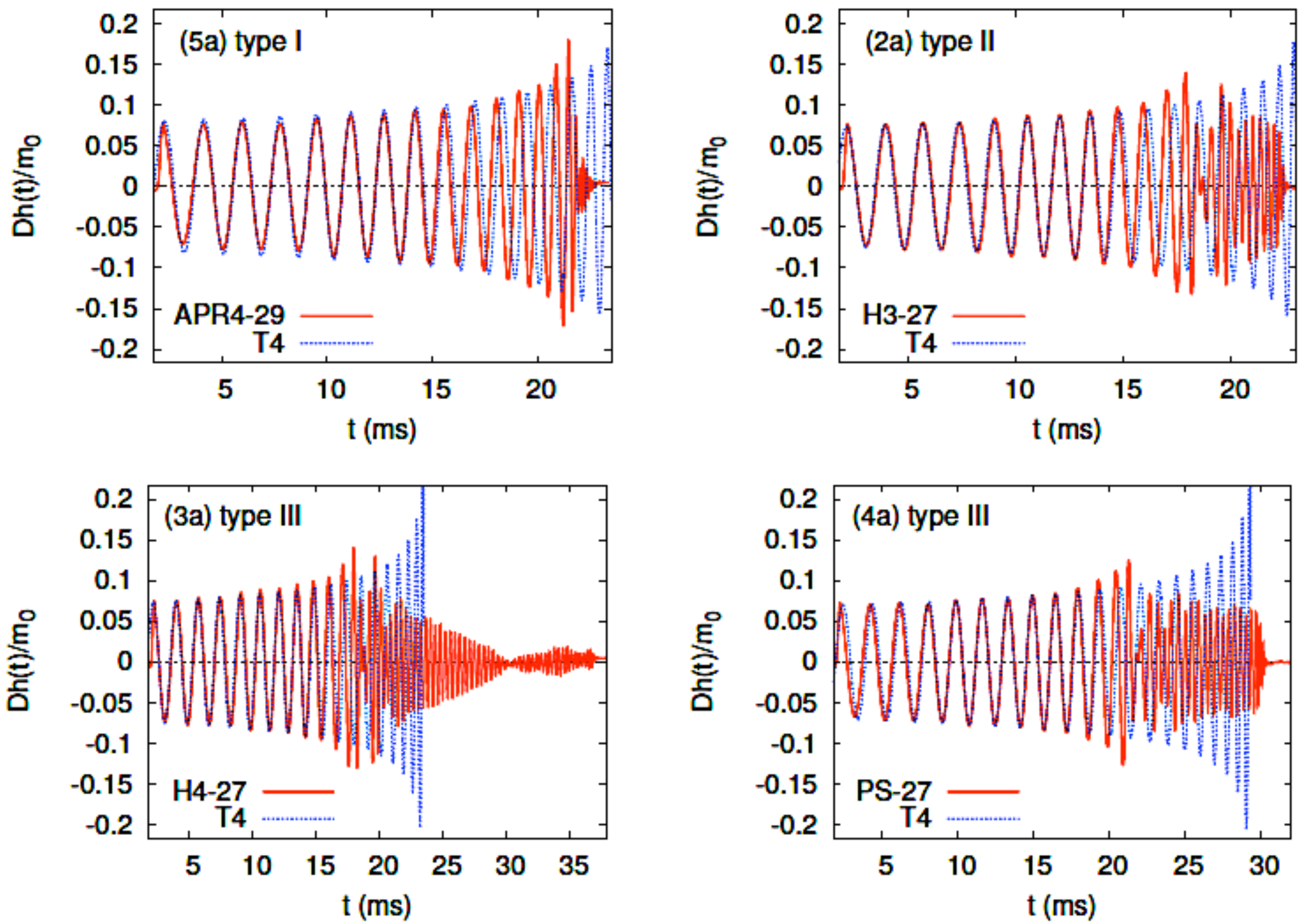

Red: Numerical Relativity
Blue: enhanced Post-Newtonian

Hotokezaka et al (2011)

Fourier spectrum (h_{eff} @ 100 Mpc)

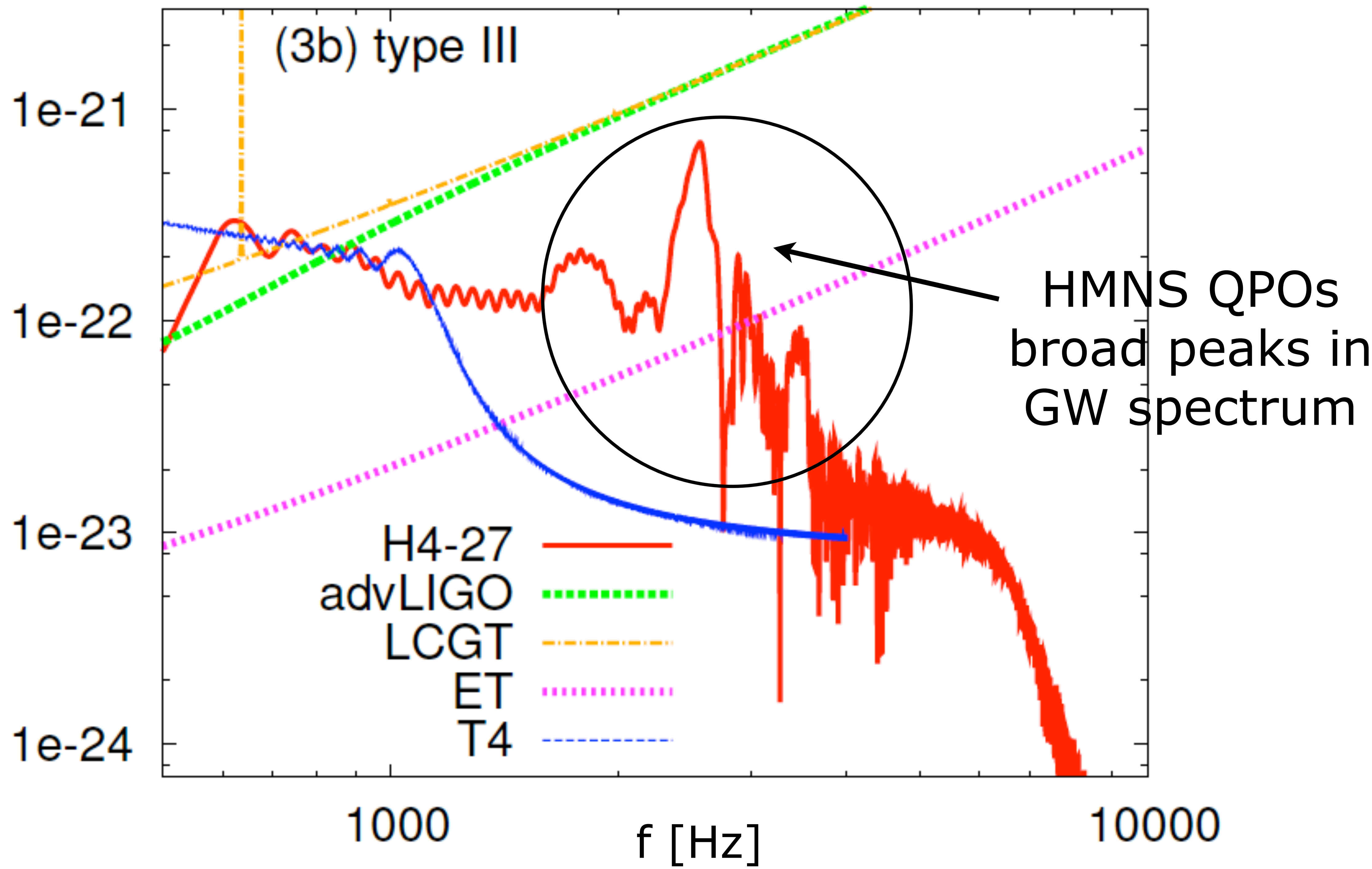

2-4 kHz peaks in spectrum detectable by 3rd generation detectors (ET) or advLIGO if source closer (20 Mpc)

Hotokezaka et al (2011)

Thermal EOS + hyperons - imprints on GWs

Weak interaction processes and neutrino cooling with GR leakage scheme. Shen EOS and thermal EOS including hyperons.

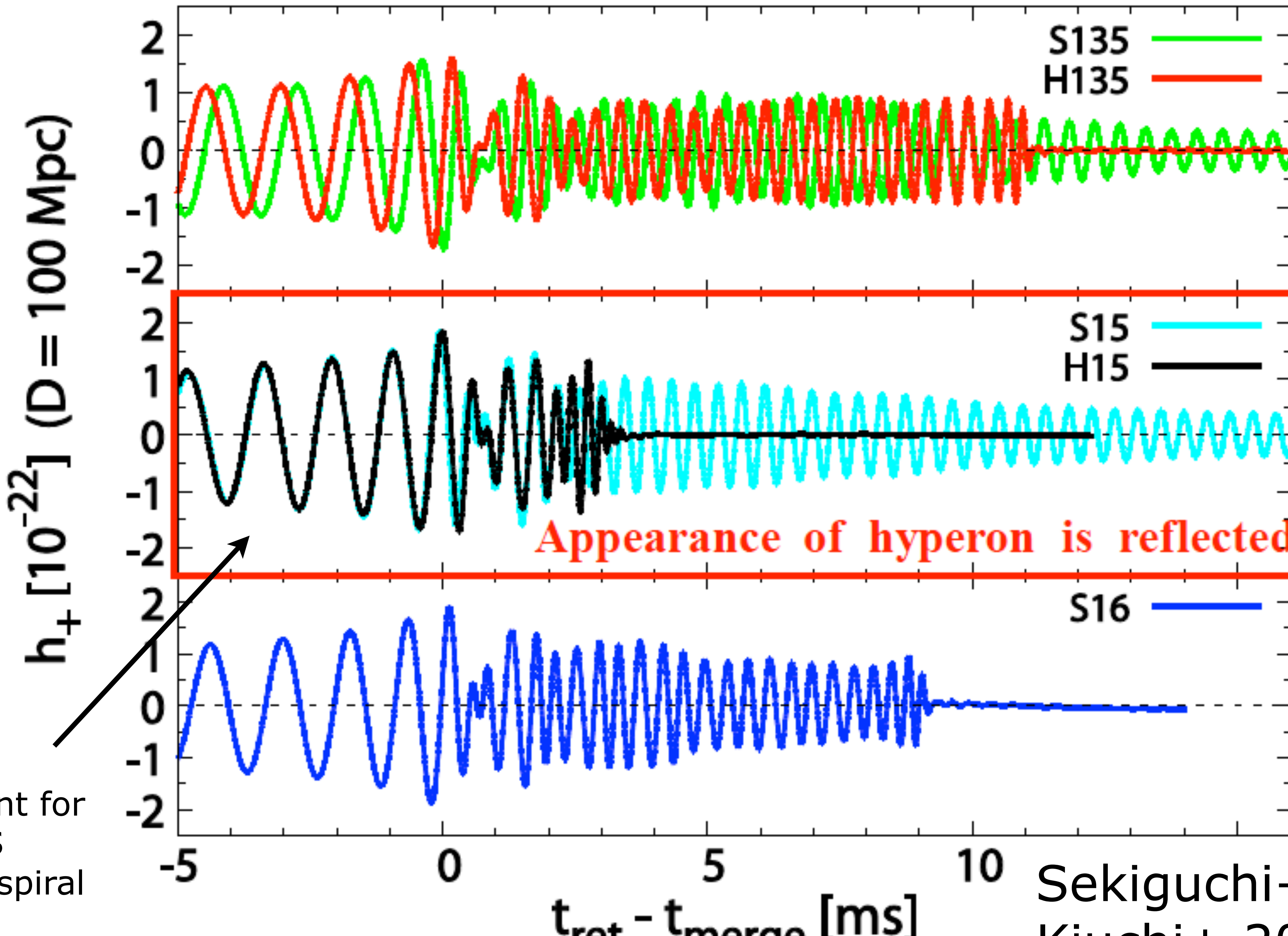

agreement for both EOS during inspiral

Sekiguchi+ 2011
Kiuchi+ 2012

NR vs AR: EOB/NR waveforms comparison

Comparison between waveforms computed from a tidal-completed EOB analytical model (Damour & Nagar 2010) and BNS simulations, comprising about 20 GW cycles of inspiral (Baiotti+ 2012).

To measure the influence of tidal effects useful to consider the phase acceleration as a function of GW frequency.

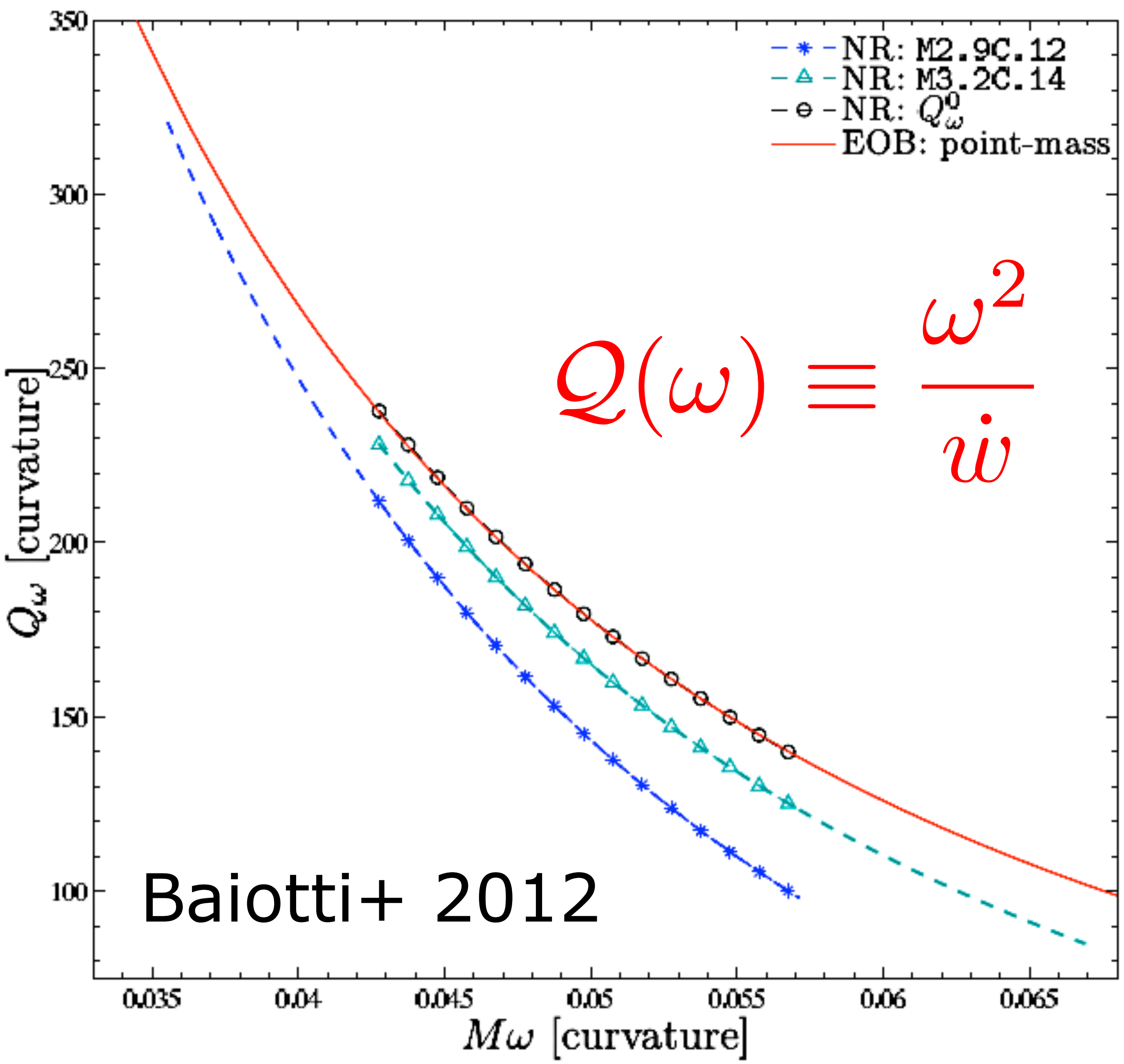

Subtraction of tidal effects from numerical relativity Q(w) curves (black empty circles) vs the corresponding point-mass EOB curve.

Excellent agreement.

Accumulated phase-diference between both curves is about -0.03rad (within accuracy needed to constraint NS radii to a good precision).

Unequal-mass BNS merger

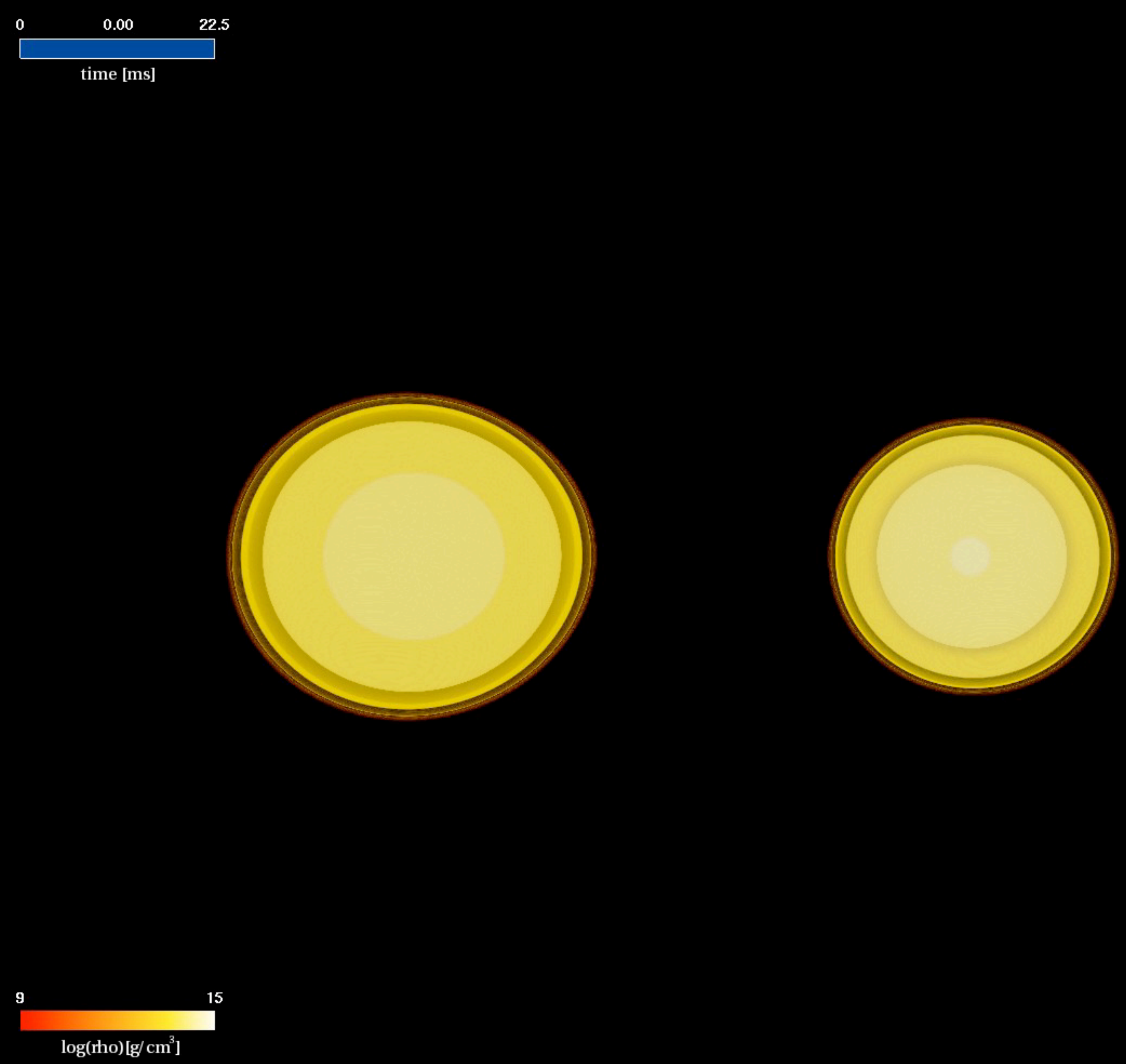

A significantly more massive torus is formed in this case.

(Rezzolla, Baiotti, Giacomazzo, Link & Font 2010)

Morphological differences (at end of simulation)

q=1.0 q=0.7

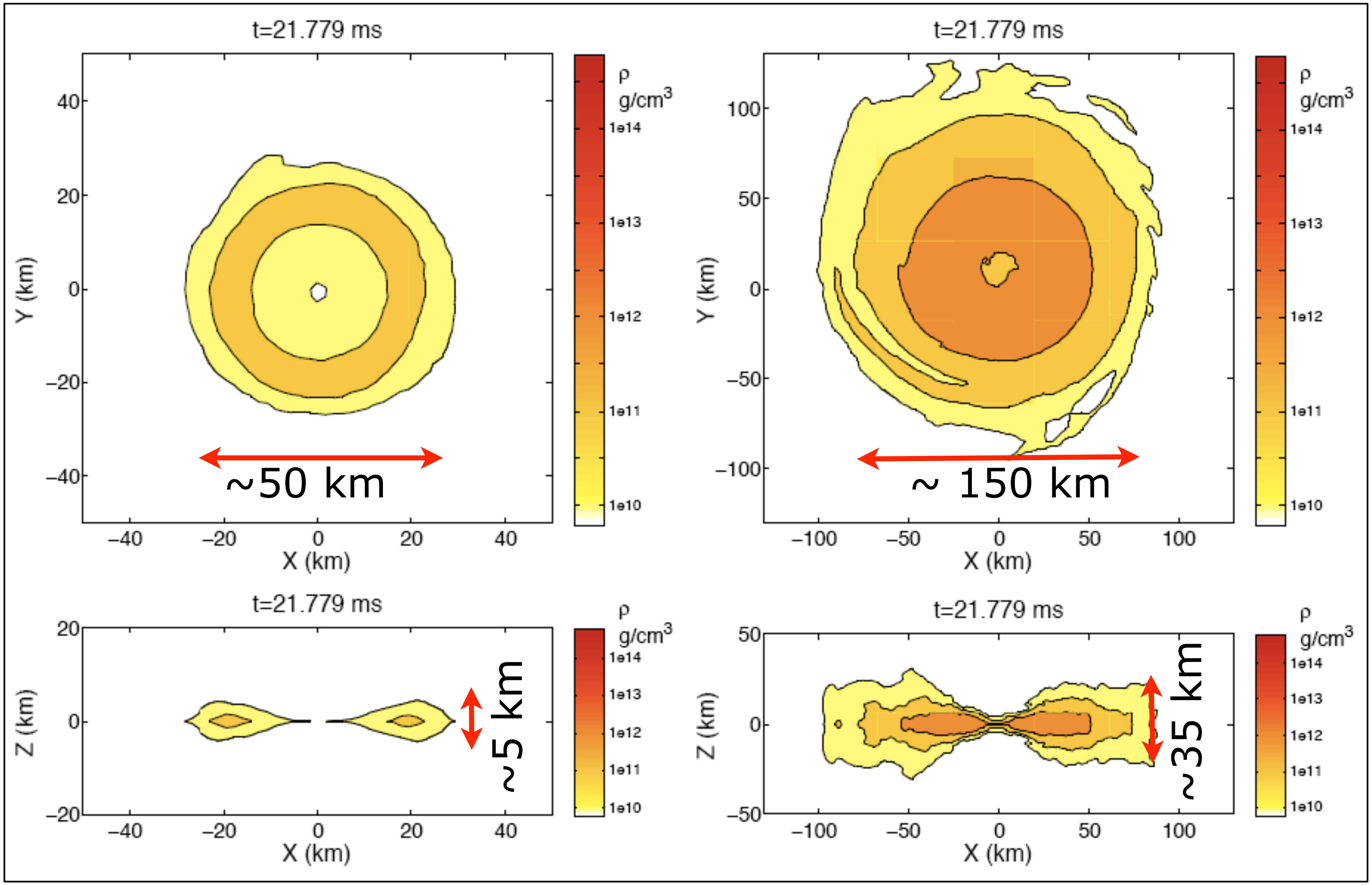

Symmetric. Thin disk. Axisymmetric shape. Thick disk.

Both tori differ in size by a factor ~3 and in mass by a factor ~200.
However, have comparable mean rest-mass densities.

Evolution of total rest mass

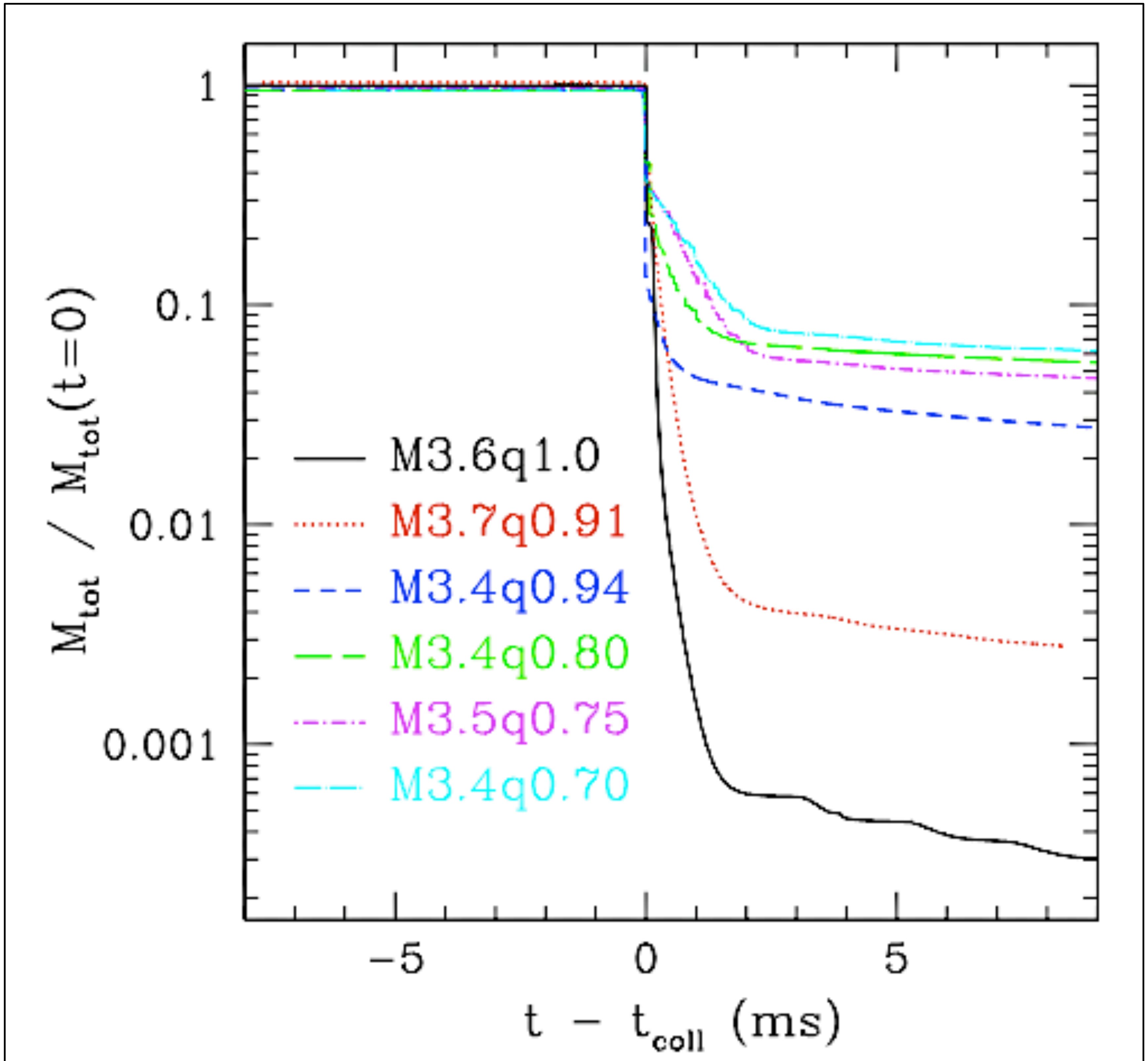

Curves shifted in time to coincide at collapse time.

Mass of resulting disk larger for smaller values of *q*.

Trend not entirely monotone; also influenced by initial total baryonic mass of binary.

Model
M3.6q1.00
M3.7q0.94
M3.4q0.91
M3.4q0.80
M3.5q0.75
M3.4q0.70

Unequal mass BNS: waveforms and PSD

Different amplitude evolution. QNM **ringdown signal** starts increasingly early for low-q binaries. (Its signature in the waveform **less evident** due to mass accretion.) Mass asymmetry also results into **different phase evolution**; may provide information on the EOS.

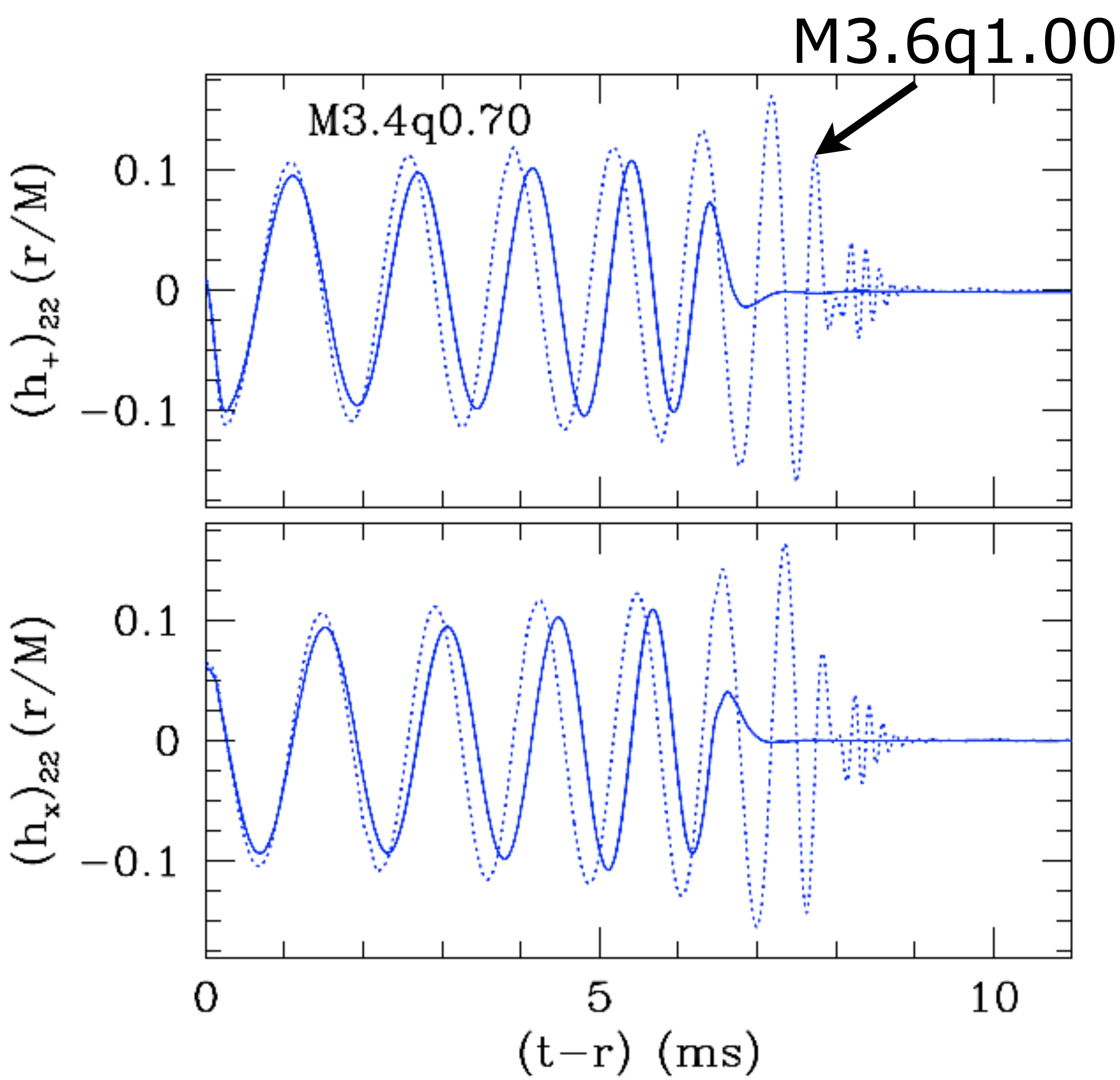

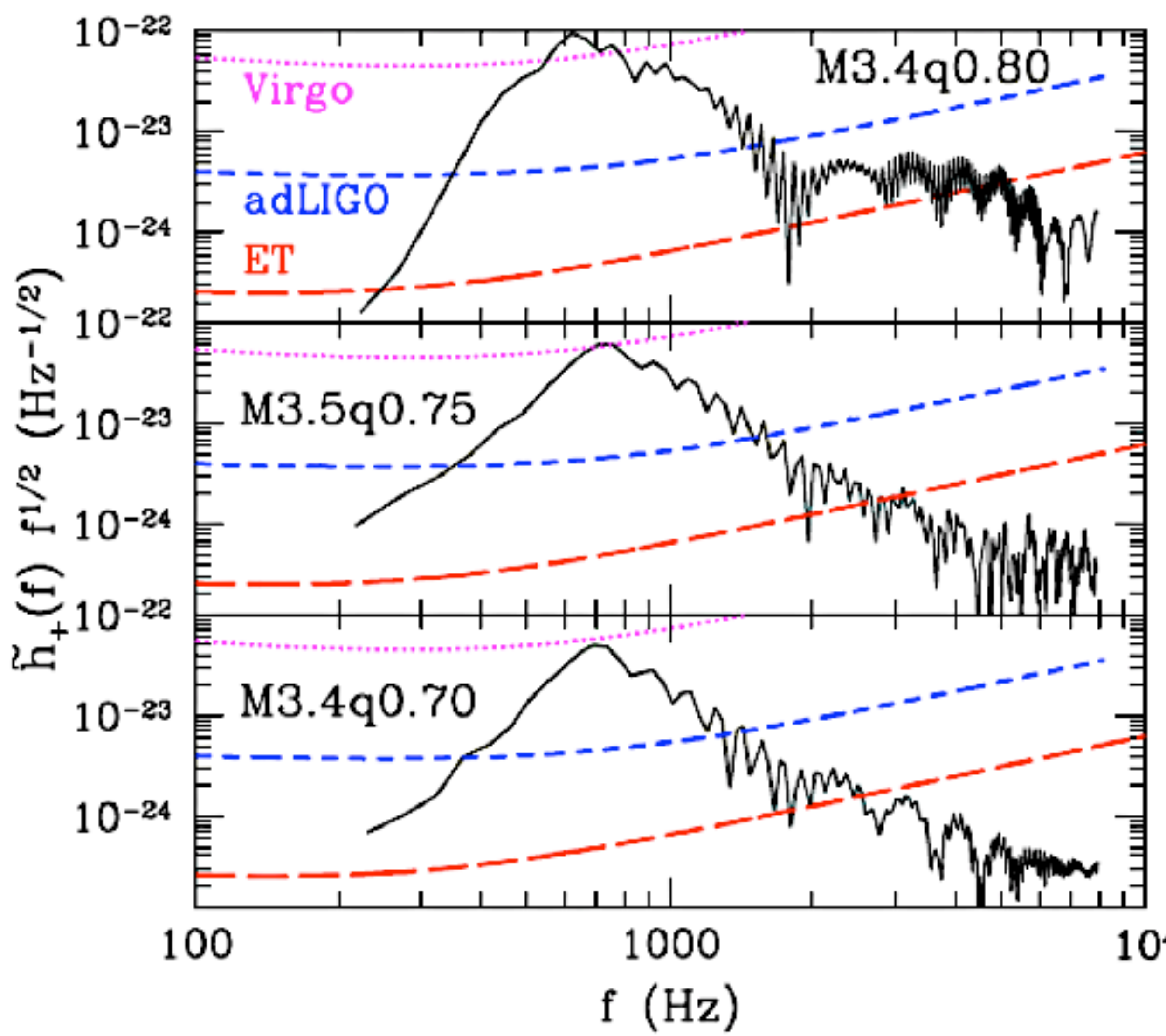

Maximal amplitude for high-q binaries; above the noise curve for Virgo. advLIGO able to reveal the inspiral signal in the interval ~ 0.3 − 2.0 kHz; all of the late-inspiral and merger signal accessible to ET.

Magnetised BNS merger (Rezzolla+ 2012)

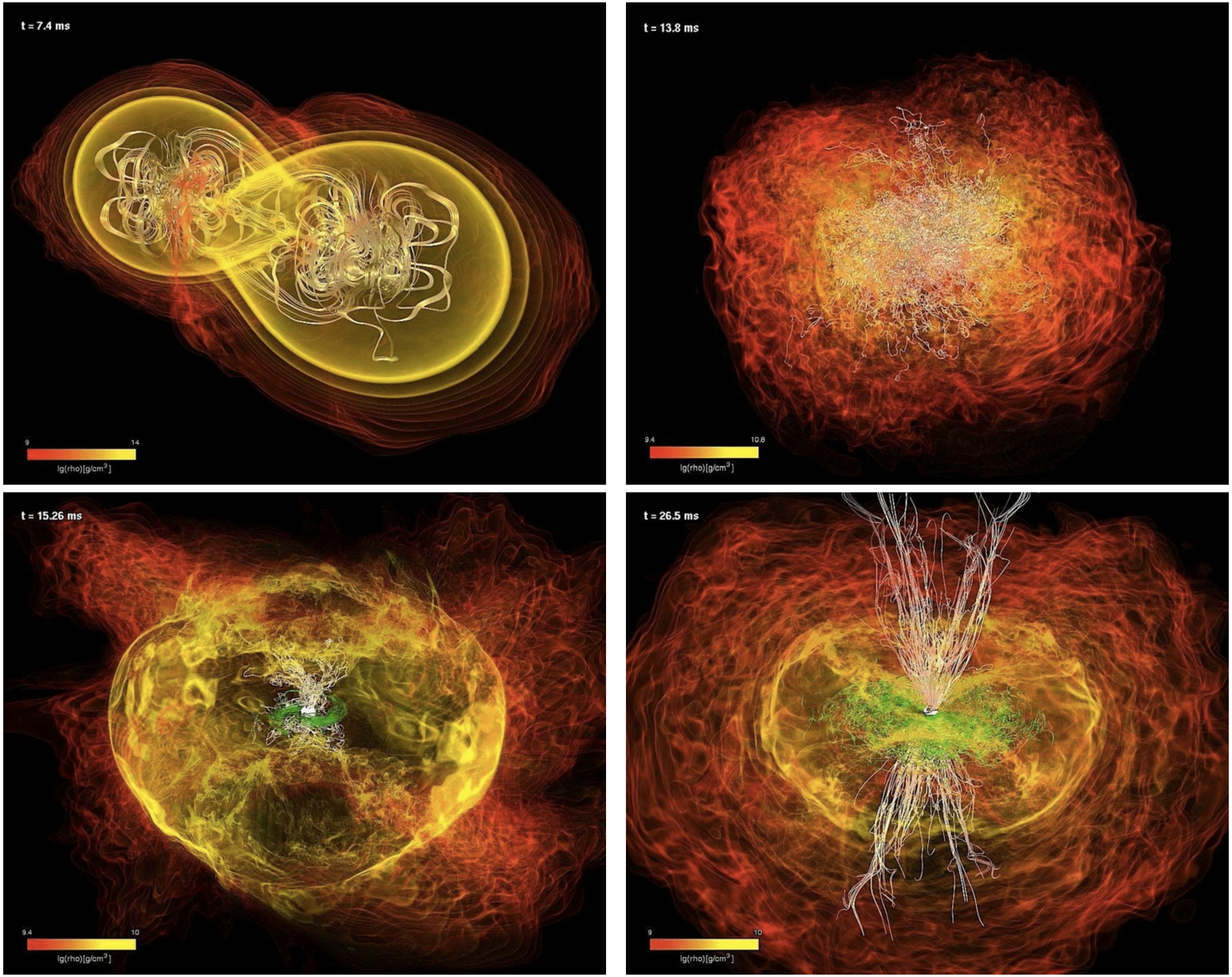

Ab-initio self-consistent formation of polar outflows from MHD effects

Black hole + accretion torus system

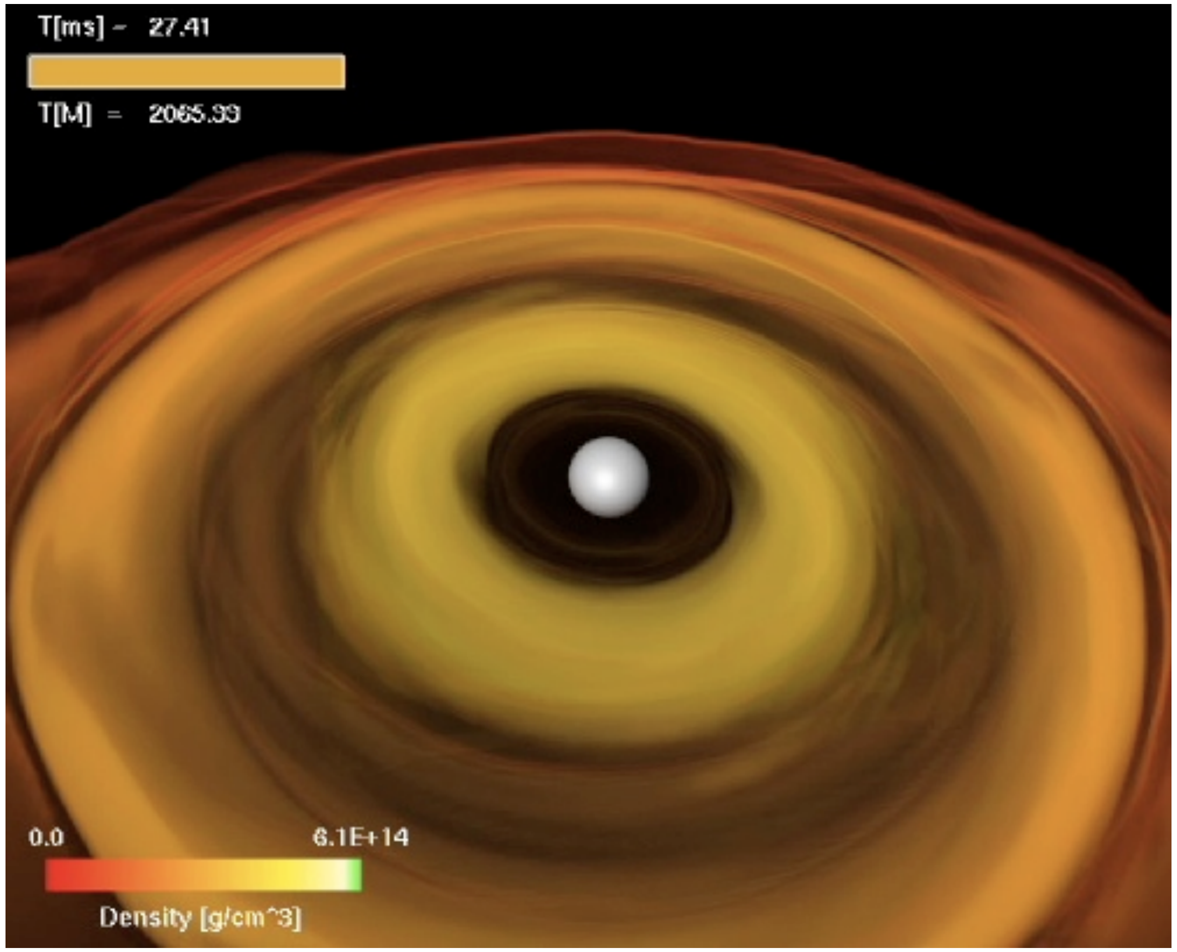

Formation and evolution of BH-torus systems not yet observed; sites opaque to EWs due to their intrinsic high density and temperature.

GWs much more transparent than EWs with respect to absorption and scattering with matter.

If BH-torus systems emitted detectable GWs, it would be possible to explore their formation and evolution, along with the **prevailing hypotheses that associate them to GRB engines.**

GRB hypothesis requires a **stable enough system to survive for a few seconds** (Rees & Meszaros 1994). Any instability which might disrupt the system on shorter timescales, such as the runaway instability and the Papaloizou-Pringle instability, could pose a severe problem for the accepted GRB models.

The runaway instability (e.g. Font & Daigne 2002)

Recent numerical relativity simulations have shown that **the runaway instability does not have a significant impact on the dynamics.**

- 2D axisymmetric: equilibrium ID. Stable tori irrespective of angular momentum distribution (Montero, Font & Shibata 2010)
- 3D: ID resulting from BNS simulation (Rezzolla et al 2011)

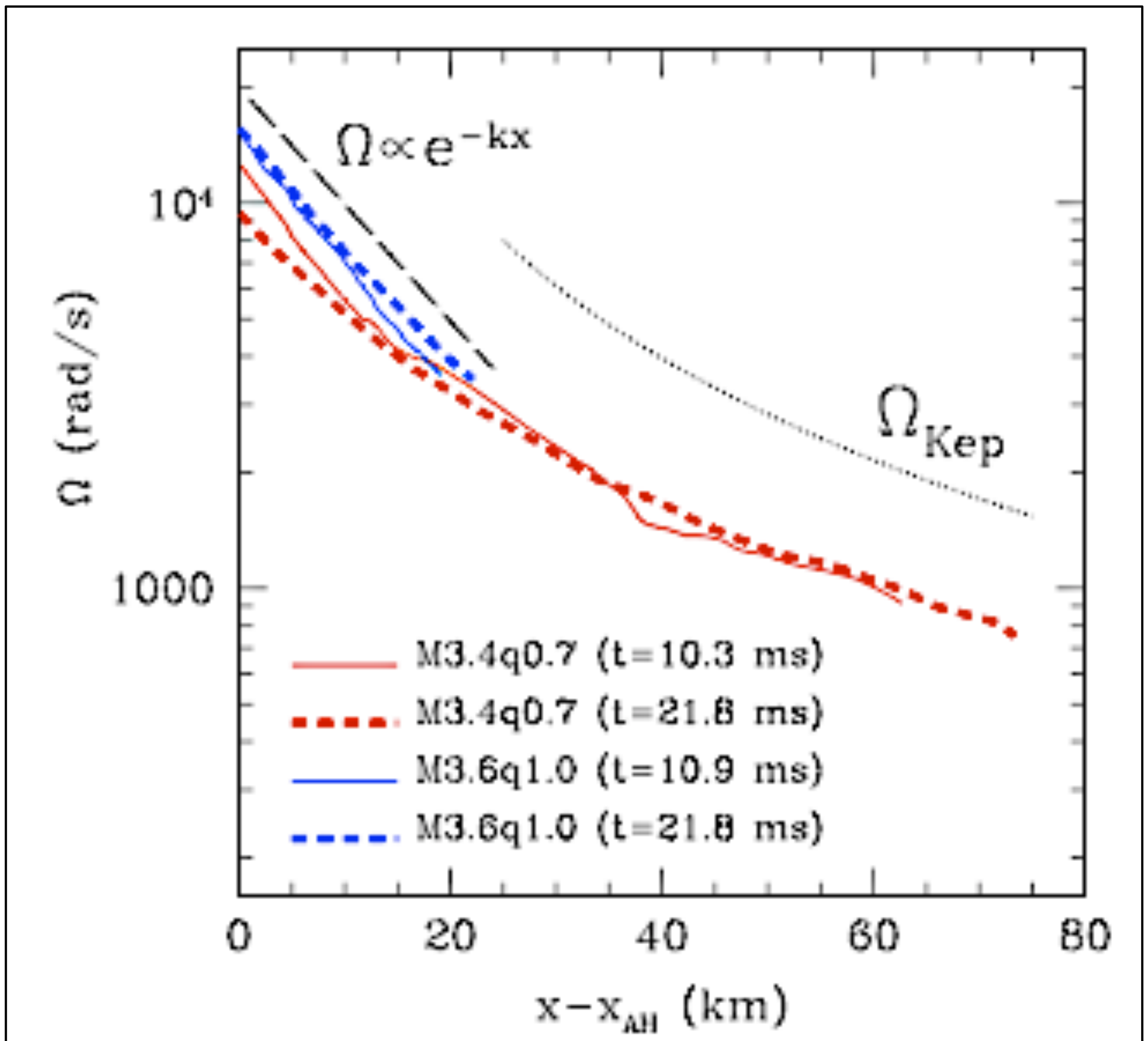

Rezzolla+ 2011

Unequal-mass binary reaches a **Keplerian** profile, $x^{-3/2}$. Explains scaling of specific angular momentum as $x^{1/2}$ and provides **firm evidence that tori produced self-consistently are dynamically stable.**

Note: Assuming *constant* specific angular momentum leads to runaway unstable disks (Korobkin+ 2013). Validity of assumption uncertain.

On longer timescales m=1 PP-instability sets in.

Korobkin+ 2011, Kiuchi+ 2011
(l-constant) (power-law)

Papaloizou-Pringle instability in tori

Papaloizou and Pringle (1984): tori with constant specific angular momentum unstable to non-axisymmetric global modes. Perturbation theory.

Basic idea: Global unstable modes have a co-rotation radius within the torus, located in a narrow region where waves cannot propagate. This region separates inner and outer regions where wave propagation is possible. Waves can tunnel through corotation zone and interact with waves in the other region. Transmitted modes amplified only if there is a feedback mechanism, in the form of a reflecting boundary at the inner and/or outer edge of the torus.

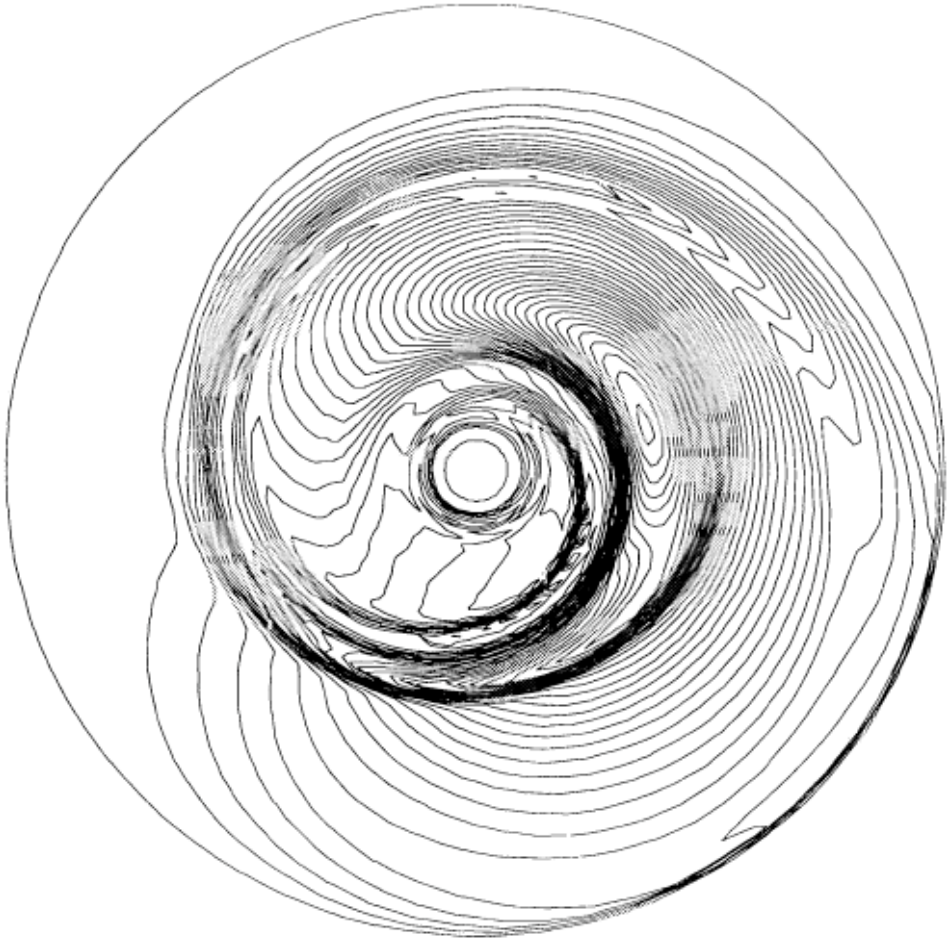

Manifestation of the PPI: counter-rotating epicyclic vortices, or **"planets"**, with m planets emerging from the growth of a mode of order m.

Early non-linear work by Hawley, Blaes, et al. Fixed metric computations.

Hawley (1991)

Animation model NC1: x-y plane

Development of the m=1 PPI

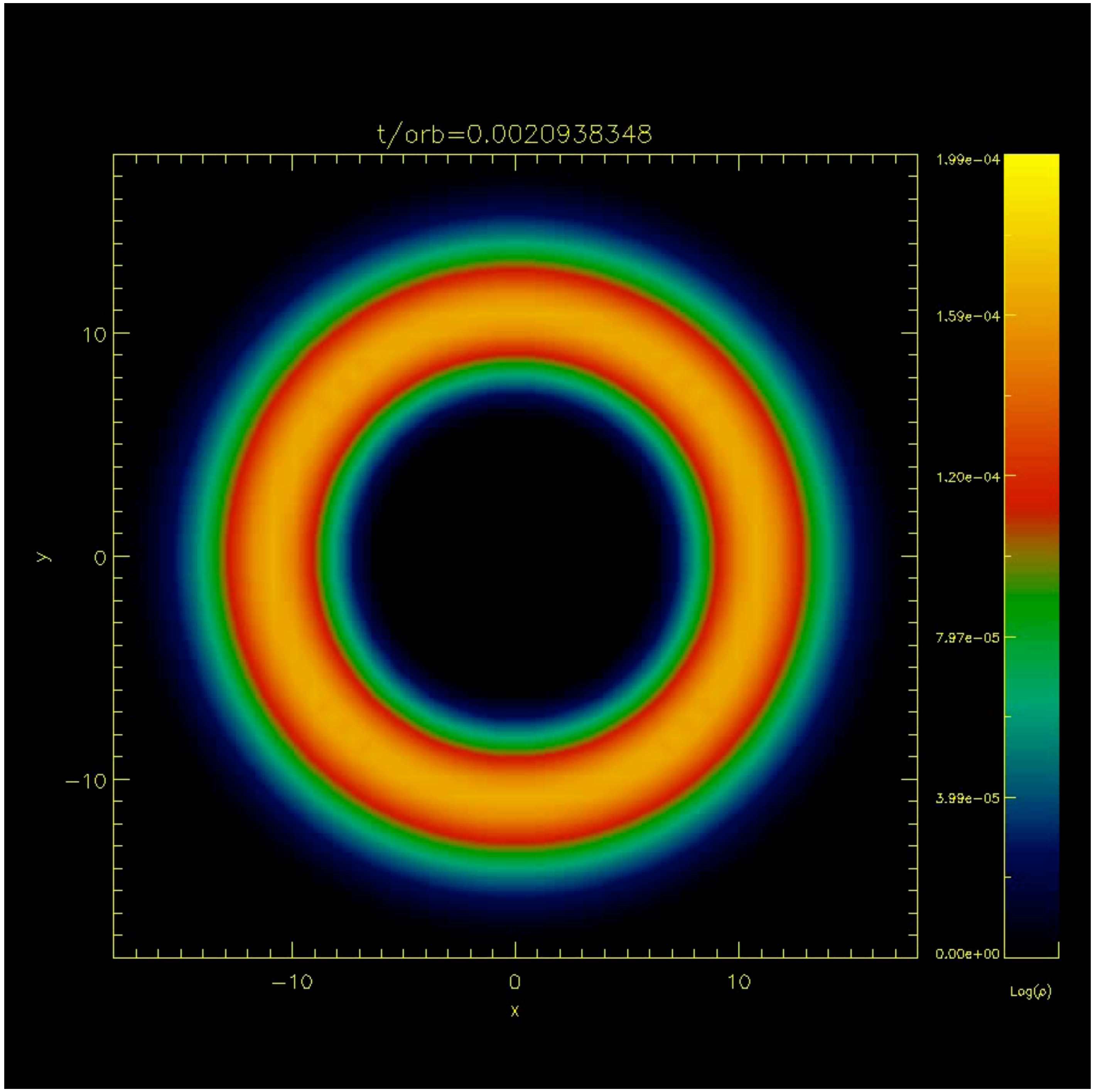

Full NR simulations.

Initial data built following the approach by Shibata (2006). Both constant and non-constant angular momentum tori.

Evolved using fixed mesh refinement NR code **SACRA** (Yamamoto, Shibata & Taniguchi 2008)

Kiuchi, Shibata, Montero & Font (2011)

m=1 mode grows for all j profiles

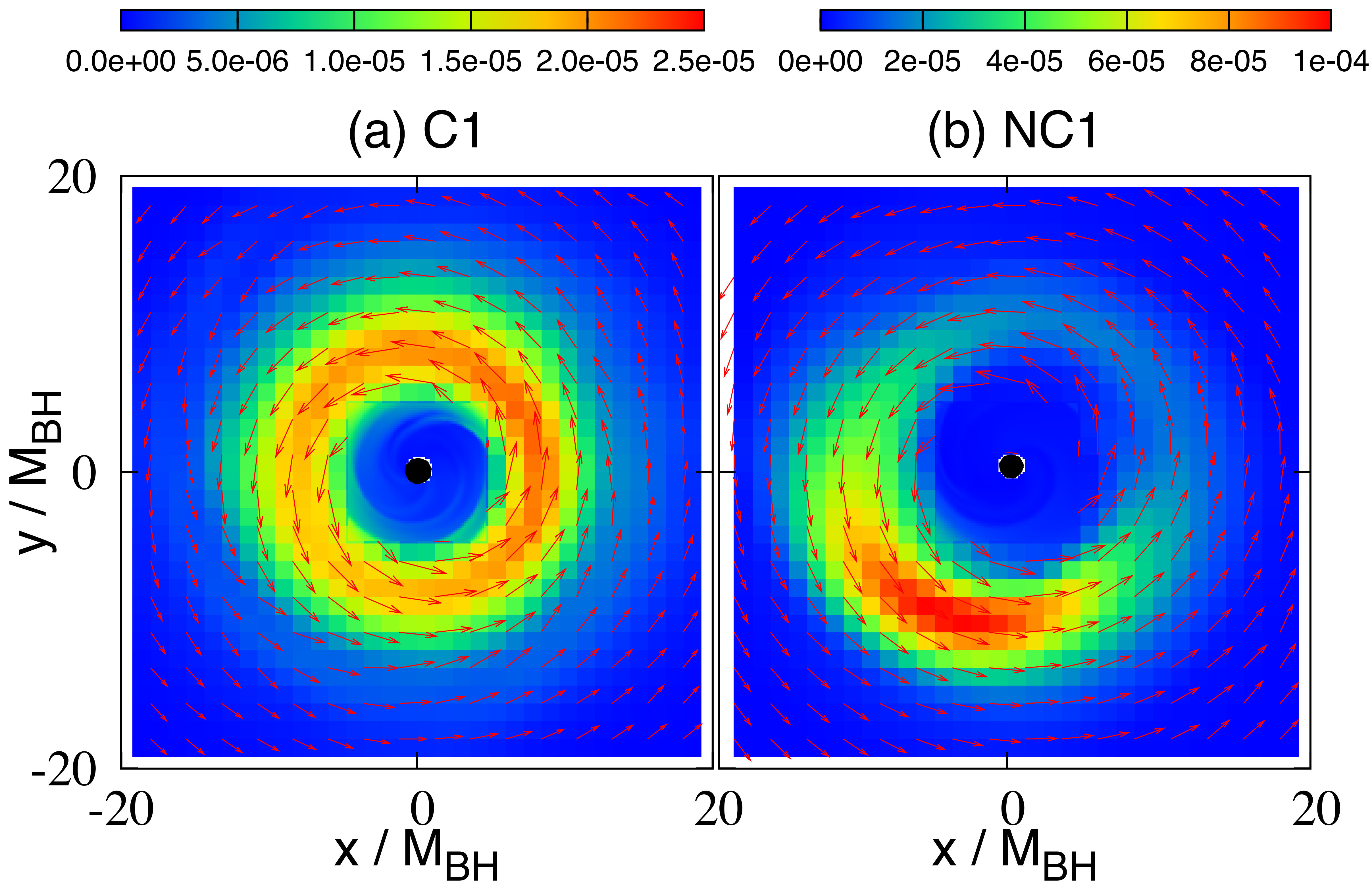

Evolution of (m=1-3) Fourier mode-amplitude

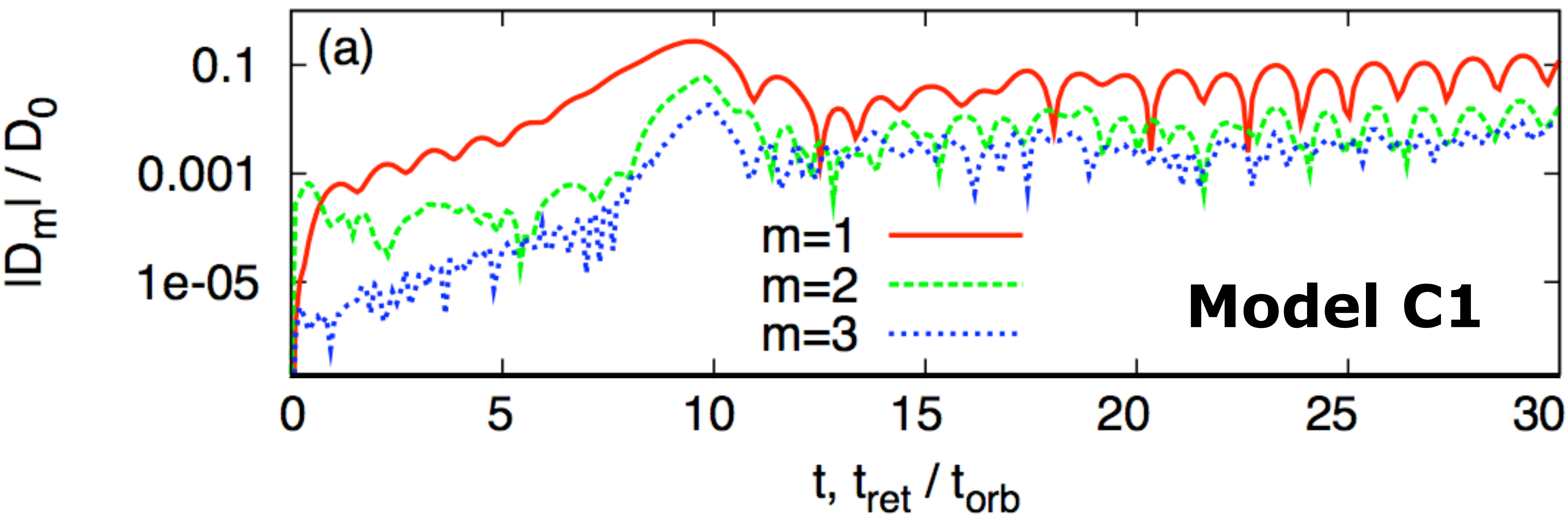

Evolution of the Fourier modes for the density perturbation of model C1.

$$D_m = \int \rho \, e^{im\varphi} \, d^3x$$

The m=1 mode is the fastest growing mode.

PPI growth rate (fit to the numerical data): $\mathrm{Im}(\omega_1)/\Omega_\mathrm{c} = 0.236$

For all models growth rate range spans 5-25% of the angular velocity.

Massive and/or j-const models show larger growth rates (agreement with Korobkin et al (2011).

Gravitational waveform

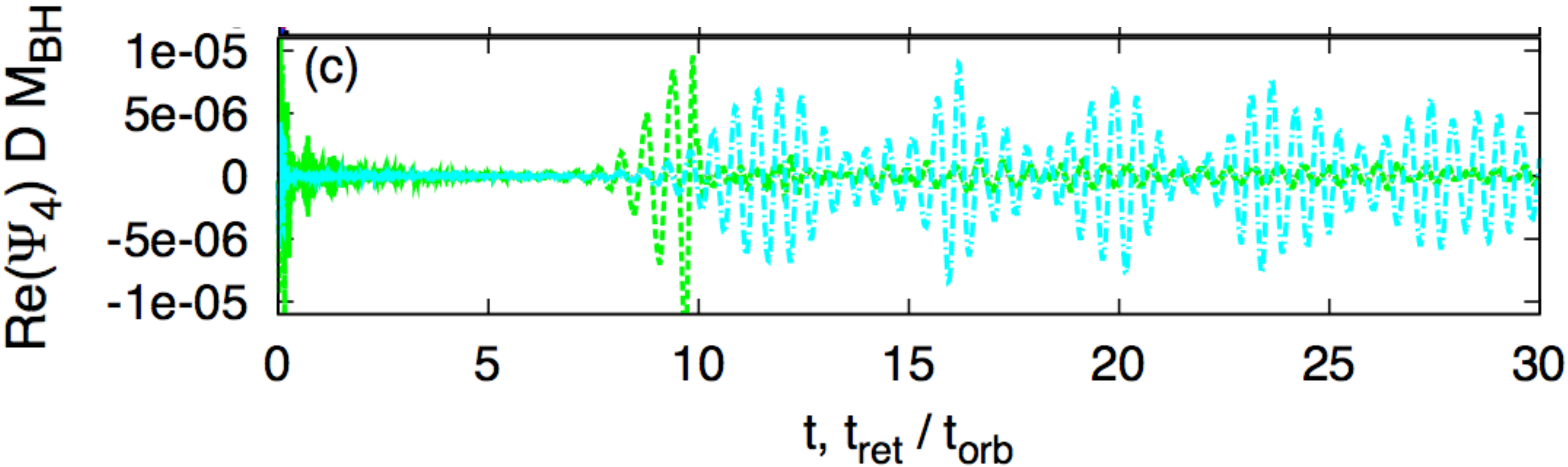

Outgoing component of the complex Weyl scalar for models **C1 (green)** and **NC1 (blue).**

Irrespective of mass ratio and rotation-law, the PPI saturates after about 10 orbital periods. Burst in GWs emitted by the PPI nonlinear growth and saturation. **After saturation, m=1 structure survives for many rotation periods and tori become good GW emitters.**

Modulation in the GW signal found for non-const j models: variability in the maximum rest-mass density and associated ***p*-mode excitation in the torus.**

Gravitational wave spectra

$M_{\rm BH} = 10^6 M_\odot, \;\; D = 10\,{\rm Gpc}$ $\qquad$ $M_{\rm BH} = 10 M_\odot, \;\; D = 100\,{\rm Mpc}$

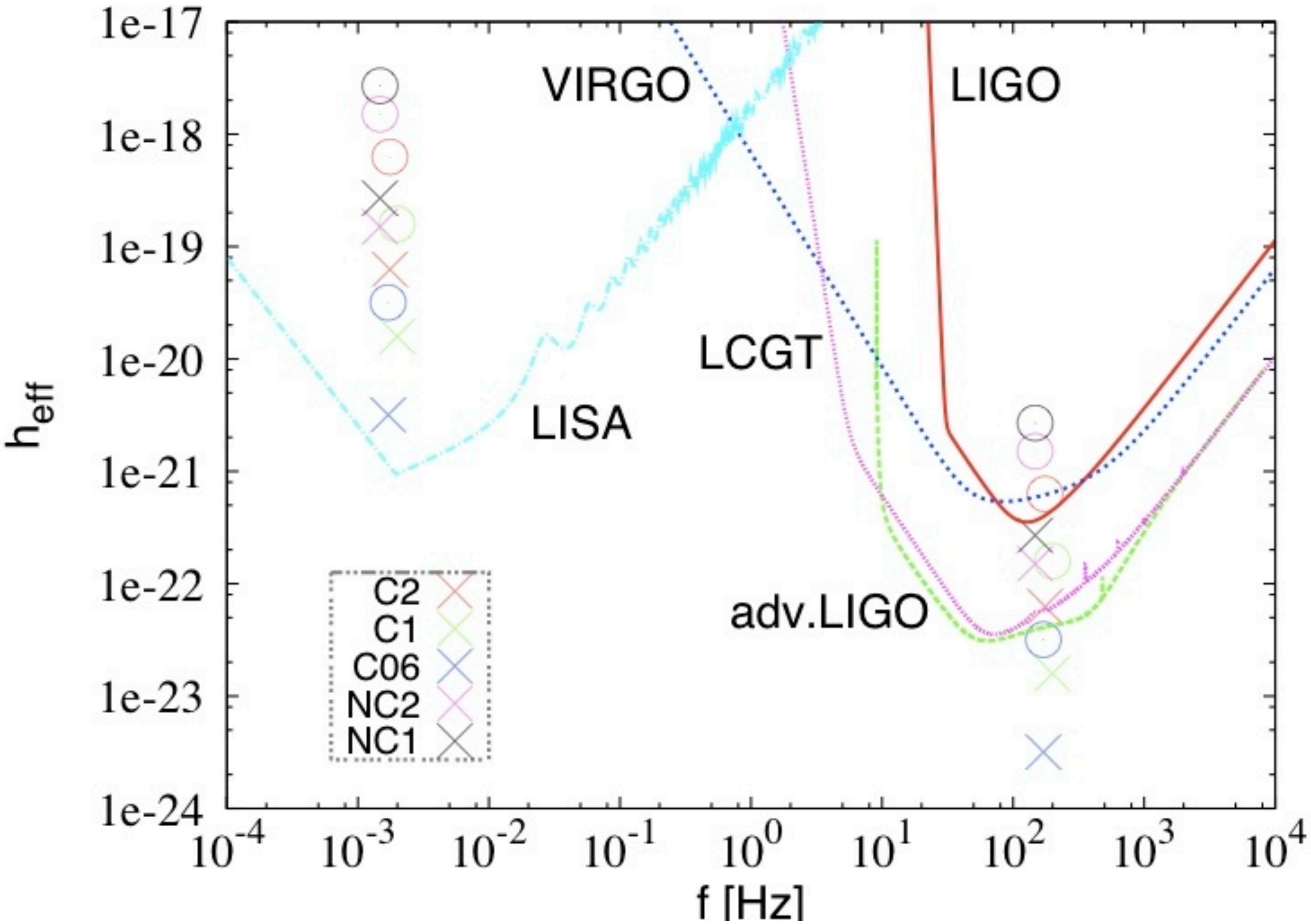

Numerical results can be rescaled for arbitrary BH mass.

X: peak amplitudes (simulations)
O: hypothetical amplitudes from accretion timescales

$t_{\rm acc} \sim 1 - 8 \times 10^4\, M_{\rm BH}$

The amplitude of the enhanced peaks could be larger than the noise level of the advanced ground-based detectors.

GWs from the SMBH scenario particularly well suited for LISA.

Summary

NR BNS simulations are ~1 decade old and coming of age.

NR simulations of BNS and black hole-torus systems presented. Focus of attention on the **GWs from the merger** and from **long-term evolution of the torus.**

GWs from BNS mergers show strong dependence on total mass and EOS. Carry imprints of specific physical features of the system.

Unequal mass BNS mergers lead to massive tori ($M \sim 0.1 M_{tot}$)

No evidence of runaway instability in non-constant angular momentum tori. On longer timescale long-lived, non-axisymmetric PP instabilities set in, **m=1 being the fastest growing mode. Leads to the emission of quasi-periodic GWs of large amplitude.**

Advanced detectors may reveal such GW source. For stellar-mass BHs our results suggest that the so-called collapsar hypothesis of GRBs may be verified via observation of GWs.